Title

Non-classical Behavior of BZT Gas in Isentropic Quasi-One-Dimensional Flow

Author

Zeng, Jingyi

Publication Date

2019

UNIVERSITY OF CALIFORNIA,
IRVINE

Non-classical Behavior of BZT Gas in Isentropic Quasi-One-Dimensional Flow

THESIS

submitted in partial satisfaction of the requirements
for the degree of

MASTER OF SCIENCE

in Mechanical and Aerospace Engineering

by

Jingyi Zeng

Thesis Committee:
Professor Feng Liu Irvine, Chair
Professor William Sirignano
Professor Dimitri Papamoschou

2020

TABLE OF CONTENTS

LIST OF FIGURES

LIST OF TABLES

NOMENCLATURE

A = cross-sectional area, m^2

a = measure of the average attraction between particles, $Pa \cdot m^6/kg^2$

b = the volume excluded by a mole of particles, m^3/kg

c = speed of sound, m/s

c_v = heat capacity at constant volume, J/K

c_p = heat capacity at constant pressure, J/K

e = internal energy, J

Γ = fundamental derivative

γ = specific heat ratio

h = enthalpy, J

h_0 = total enthalpy/stagnation enthalpy, J

M = Mach number

M_g = Molecular weight, kg/mol

p = pressure, Pa

p_0 = total pressure/stagnation pressure, Pa

p_c = critical pressure, Pa

R = specific gas constant, $J/(kg \cdot K)$

ρ = density, kg/m^3

ρ_0 = total density/stagnation density, kg/m^3

ρ_c = critical density, kg/m^3

s = entropy, J/K

T = temperature, K

T_0 = total temperature/stagnation temperature, K

T_c = critical temperature, K

u = flow velocity, m/s

v = specific volume, m^3/kg

v_c = critical specific volume, m^3/kg

ACKNOWLEDGMENTS

I would like to express my sincere gratitude to my advisor Prof. Feng Liu for the continuous support of my graduate study and related research, for his patience, motivation, and immense knowledge. His guidance helped me in all the time of research and writing of this thesis. I could not have imagined having a better advisor and mentor for my graduate study.

Besides my advisor, I would like to thank the rest of my thesis committee: Prof. Dimitri Papamoschou and Prof. William Sirignano for their valuable guidance. You provided me with the tools that I needed to choose the right direction and successfully complete my research.

My sincere thanks also go to my fellow labmates and friends in the UCI MAE department, for the stimulating discussions, for the sleepless nights we were working together before deadlines, and for all the fun we have had in the last three years.

Last but not the least, I must express my very profound gratitude to my parents and to my boyfriend for providing me with unfailing support and continuous encouragement throughout writing this thesis and my life in general. This accomplishment would not have been possible without them. You are always there for me. Thank you.

ABSTRACT OF THE THESIS

Non-classical Behavior of BZT Gas in Isentropic Quasi-One-Dimensional Flow

by

Jingyi Zeng

Master of Science in Mechanical and Aerospace Engineering

University of California, Irvine, 2020

Professor Feng Liu Irvine, Chair

A thermodynamic property of gases called the fundamental derivative was first proposed by Bethe(1942) and later defined as the dimensionless quantity $\Gamma = \frac{c^4}{2v^3}\left(\frac{\partial^2 v}{\partial p^2}\right)_s$. The sign of Γ reflects the sign of the curvature of the isentrope in the pressure-specific volume plane. The value of Γ significantly affects the gas behavior and flow properties. Gases at relatively low pressure away from the critical pressure levels usually have values of Γ above 1.0. For an ideal gas, $\Gamma = \frac{\gamma + 1}{2}$, where γ is the ratio of specific heats. Previous studies identified flow behaviors of gases with $\Gamma < 0$ that are qualitatively opposite to classical gas dynamic theories based on perfect gas laws. For example, a divergent channel accelerates a subsonic flow and expansion shocks exist for gases with negative Γ. Although no experimental evidence has yet been found to confirm such non-classical gas flow behaviors, present interests in the use of super-critical heavy gases as well as pure academic curiosity call for more in-depth and definitive studies of such gas flows. A dense gas called MDM is selected as the working fluid in the present work. A region of negative fundamental derivative is found near the critical point using the Van der Waals real gas Equation of State (EoS) for this heavy gas. Contrary to previous studies, the present work considers Γ as a local thermodynamic variable instead of a constant in an isentropic flow or across a shock wave. Formulas of the relation of the fundamental derivative to other thermodynamic variables are given. To compare with the ideal gas model, the thermodynamic properties of this dense gas and the gas dynamic behaviors near its critical point are investigated. The conservation laws have been applied to develop the ordinary differential equation system for the quasi-one-dimensional isentropic flow. Since analytical solutions as in the classical theory are no longer possible for the non-ideal gas, numerical simulations are obtained for different upstream conditions. Various seemingly counter-classical gas dynamics flow behaviors are demonstrated. For example, a divergent-convergent nozzle is needed for transonic flow when the gas is within the negative fundamental derivative range. These unconventional gas behaviors are vitally interrelated in a flow of such non-ideal gas as it expands from high pressure to low pressure going through regions of $\Gamma > 1$, $0 < \Gamma < 1$, and $\Gamma < 0$ due to changes of its thermodynamic properties in the isentropic expansion process. Specific counter-classical behaviors are identified and discussed in this thesis.

Chapter 1

Introduction

1.1 Background

Due to recently growing attention to super-critical CO_2 power cycle in turbo-machinery [1][2][3], understanding dense gas flow and its thermal behavior near or above the critical point becomes important for improving compressor performance and engineering margins[4][5]. Besides the study of super-critical CO_2 as a working fluid, research on other non-conventional fluids and related simulations have also received attention. Different real gas equations of state are selected to achieve more accurate results, including but not limited to the Van der Waals(VdW), the Soave-Redlich-Kwong(SRK), and the Peng-Robinson(PR) equations of state. The present work focuses on the analysis of dense gas behavior in quasi-1D flow and its differences from the classical theory for the ideal gas.

Earlier studies include research on thermodynamics and transport properties of dense gas and the gas dynamic behavior near its critical point. In 1942, Bethe [6] first used the Van der Waals gas model to show that there was a finite region in the pressure-specific volume plane where the isentropes have negative curvature. When the dense gas is within this particular region, it behaves very differently from the classical analysis. Conventional perfect gas theory states that only compression shock waves are physically possible to satisfy the Second Law. Bethe[6], Duhem[7], Weyl[8], Courant and Friedrichs[9] and other researchers envisaged the possibility that rarefaction shocks might occur in single-phase vapors. Later Landau and Lifshitz [10] found a non-dimensional form of $(\partial^2 v/\partial p^2)$ to describe the gas basic behavior and defined it as the fundamental derivative Γ. In 1971, Thompson[11] showed that the sign of this non-dimensional thermodynamic quantity determined the possibility of forming rarefaction shocks in an arbitrary fluid. He stated that the existence of rarefaction shocks required negative fundamental derivative and other conditions to be satisfied. Their achievements greatly promoted the development of dense gas dynamics. To distinguish from classical gases of low molecular complexity, a particular class of dense gas called Bethe-Zel'dovich-Thompson (BZT) gas was named. BZT fluids have embedded regions of negative fundamental derivative near the critical point. Some steady transonic flow behaviors of these fluids were investigated by Cramer and Tarkenton[12].

Dense gas effects were taken into consideration in nozzle flow analyses a long time ago at the beginning of the last century by Callendar[13]. Recent studies focused more on non-ideal gas flow and its application. Sullivan[14] provided a review and comparison of five isentrope equations: the polytrope, Walker, Van der Waals, Rayleigh, and Callendar models. The historical development and limitation of each model were discussed. Arp et al.[15] attempted to find the occurrence of the Gruneisen parameter which relates thermodynamic properties to lattice vibrational spectra and has long been used in equations of state for solids[16]. Leung and Epstein[17] focused on one-dimensional isentropic flow and developed a generalized critical flow model for the non-ideal gas flow. By adopting the Redlich-Kwong (R-K) equation of state, their computation results for various common gases were compared with Johnson's work[18] as well as the experimental data. Bober and Chow[19] also did numerical computation on the convergent-divergent nozzle and obtained a method for one-dimensional non-ideal gas flow by applying the R-K equation of state. They used methane gas as working fluid and gave the plots of pressure, temperature, and area ratios as functions of Mach number. More recently, Sirignano [20][21] discussed the real-gas modifications for compressible flow at high pressures and analyzed normal compressive shock wave with supercritical upstream thermodynamic conditions using the SRK model. Calculation results for some common gases including argon, nitrogen, and carbon dioxide were presented.

Besides single component fluids, some non-conventional gas behaviors of multi-component fluids have also been discussed. Different from the mixtures of ideal gases, the molecular interactions between different molecules play an important role here, and the thermodynamic properties of dense vapours of multi-component mixtures are no longer linear functions of the mole fractions of each compound. Colonna and Silva [22] presented the procedure to evaluate the equation of state for highly non-ideal mixtures, and the fundamental derivative for Siloxanes. Angelino and Invernizzi [23] showed the experimental results on the thermal stability of siloxane mixtures. Guardone et al.[24] did a review on the non-classical gas dynamics of mixtures, and showed numerical simulations of a supersonic expansion by using mixtures of siloxanes and perfluorocarbons. They also gave the conclusion that the mixing compounds of the same fluid family does not enhance the non-classical gas dynamic phenomena for the considered mixtures. But more limitations need to be discussed.

These previous work focused more on the real gas effect and gave plenty of results for common gases. Some of the cases are for gas near its critical region but does not really fall into the negative fundamental derivative region. In contrast to their studies, the present work has selected a family of organosilicon compound as working fluid due to the relatively large region of negative fundamental derivatives associated with it, and considers the fundamental derivative as a local thermodynamic variable instead of a constant through the flow. A complete set of theories for non-classical behavior of BZT gases including the general relation of the fundamental derivative to other thermodynamic variables are given.

1.2 Study Approach

For dense gas flow, the ideal-gas equation of state and many thermodynamic relations based on the ideal gas law are no longer valid when inter-molecular-forces within the fluid become important. The differences between the ideal gas and real gas behaviors need to be understood. In particular, it is necessary to develop a set of theories for non-classical gas flow. Later it can be applied to quasi-one-dimensional nozzle flow to identify trends in the gas dynamic behavior that are not observed in classical ideal gas flow theory. It is also important to locate the region where the fluid exhibits negative fundamental derivative. Once the specific regions are located, numerical simulation methods could be applied to analyze the flow behavior in this area and to capture unconventional gas dynamic behavior such as possible rarefaction shocks and compression fans. The specific gas behavior analysis and the corresponding thermodynamic relations should be derived from basic conservation laws and the real gas equation of state.

In the present work, the Van der Waals gas model is selected for numerical computation. The Van der Waals EoS is used for its simplicity without loss of generality in uncovering the non-classical behaviors of the BZT gas. The region of negative fundamental derivative is located, and non-classical gas behaviors within this particular region are discussed, including the expressions of thermodynamic properties, the relation between Mach number and flow velocity, and the area variation of a transonic passage, etc. The isentropic exponents used by previous researchers to describe the real gas effect are mentioned, and discussions on why the isentropic exponents are not used in the present work are given. How the fundamental derivative is related to other thermodynamic variables are discussed, and the corresponding thermodynamic relations in isentropic quasi-one-dimensional flow are derived. To show the non-classical gas behaviours intuitively, a dense gas called MDM from the siloxanes family is used in this thesis. Several cases of isentropic flow were run on our in-house code and the results are presented here.

Chapter 2

The Fundamental Derivative of Gases

2.1 Definition of the Fundamental Derivative

The definition of the fundamental derivatives and why it is so important in dense gas dynamics have been discussed by Landau and Lifshitz[10] and Thompson[11]. From their theory, the non-dimensional form of Γ is given as

$$\Gamma = \frac{c^4}{2v^3}\left(\frac{\partial^2 v}{\partial p^2}\right)_s \tag{2.1}$$

where c is the speed of sound, v is specific volume, p is pressure and the subscript s means the derivative is taken at constant entropy s.

2.2 Other Expressions for the Fundamental Derivative

From the definition above, the sign of Γ is related to the term $\left(\frac{\partial^2 v}{\partial p^2}\right)_s$ directly. Also, no matter which gas model is used for analysis, there is no doubt that the behavior of a gas is associated with the curvature of the isentrope in the $p - v$ plane, measured by $\left(\frac{\partial^2 v}{\partial p^2}\right)_s$. For a better understanding of the relationship between Γ and the unconventional dense gas behavior, the first step is to rearrange the equation and to express Γ in terms of other thermodynamic variables.

For general equations of state, the speed of sound c is given by

$$c^2 = \left(\frac{\partial p}{\partial \rho}\right)_s = -v^2 \left(\frac{\partial p}{\partial v}\right)_s \geq 0 \tag{2.2}$$

Notice

$$\left(\frac{\partial v}{\partial p}\right)_s = \frac{1}{\left(\frac{\partial p}{\partial v}\right)_s} \tag{2.3}$$

Thus

$$\left(\frac{\partial^2 v}{\partial p^2}\right)_s = \frac{\partial}{\partial p}\left[\frac{1}{\left(\frac{\partial p}{\partial v}\right)_s}\right]_s = \frac{\partial}{\partial v}\left[\frac{1}{\left(\frac{\partial p}{\partial v}\right)_s}\right]_s \frac{1}{\left(\frac{\partial p}{\partial v}\right)_s} = -\frac{\left(\frac{\partial^2 p}{\partial v^2}\right)_s}{\left(\frac{\partial p}{\partial v}\right)_s^3} \tag{2.4}$$

Substituting above into Equation (2.1) and making use of Equation (2.2), we obtain

$$\Gamma = \frac{v^3}{2c^2}\left(\frac{\partial^2 p}{\partial v^2}\right)_s \tag{2.5}$$

Equation (2.5) is used more generally than the original definition due to the common form of polynomial equation of state. Typically pressure is given as a function of other thermodynamic variables and thus it would be easier to derived the expression of $\left(\frac{\partial^2 p}{\partial v^2}\right)_s$ than the expression of $\left(\frac{\partial^2 v}{\partial p^2}\right)_s$. Equation (2.5) states that Γ is related to the curvature of the isentrope. Under most conditions, the isentrope is a concave curve in the $p - v$ diagram. So conventionally Γ is supposed to be positive. For a dense gas, there can be a region near the saturation line where Γ turns negative.

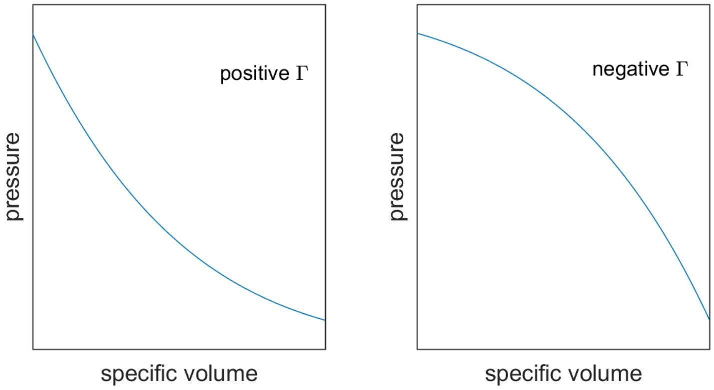

Figure 2.1: Sign of the fundamental derivative

Besides the sign of Γ, another variable to be concerned about is the speed of sound, which is tightly coupled with Γ. The second-order partial derivative in equation (2.5) can be expressed in terms of density and the speed of sound

$$\left(\frac{\partial^2 p}{\partial v^2}\right)_s = \left(\frac{\partial}{\partial v}\left(\frac{\partial p}{\partial v}\right)_s\right)_s = \left(\frac{\partial}{\partial v}\left(-\frac{c^2}{v^2}\right)\right)_s = \frac{1}{v^2}\left(\frac{\partial(\rho c)^2}{\partial \rho}\right)_s = \frac{2c}{v^3}\left(\frac{\partial(\rho c)}{\partial \rho}\right)_s \tag{2.6}$$

which shows directly the relationship between the sound of speed and Γ

$$\Gamma = \frac{1}{c}\left(\frac{\partial \rho c}{\partial \rho}\right)_s = 1 + \frac{\rho}{c}\left(\frac{\partial c}{\partial \rho}\right)_s = 1 - \frac{v}{c}\left(\frac{\partial c}{\partial v}\right)_s \tag{2.7}$$

Consider an expansion process. When the gas is within $\Gamma < 1$ region (non-classical gas), equation (2.7) states that the speed of sound increases as density decreases, under isentropic condition.

In addition to density variations, a compression or expansion process is usually reflected by pressure change. Note

$$\left(\frac{\partial \rho c}{\partial \rho}\right)_s = c + \rho\left(\frac{\partial c}{\partial \rho}\right)_s = c + \frac{1}{v}\left(\frac{\partial c}{\partial p}\right)_s\left(\frac{\partial p}{\partial \rho}\right)_s = c + \frac{c^2}{v}\left(\frac{\partial c}{\partial p}\right)_s \tag{2.8}$$

Substituting it back into equation (2.7), we obtain

$$\Gamma = 1 + \frac{c}{v}\left(\frac{\partial c}{\partial p}\right)_s \tag{2.9}$$

Equations (2.1), (2.5), (2.7), (2.9) are four different but equivalent expressions for the fundamental derivative Γ in terms of different thermodynamic properties, each of which shows a significant physical insight into the meaning of Γ. There are two demarcation lines that are relatively important in this analysis. For a perfect gas whose isentropic process can be expressed as $pv^\gamma = const$, it is easy to show $\Gamma = \frac{1+\gamma}{2} > 1$, which would be the case with a conventional gas under normal conditions. When $\Gamma > 1$, the speed of sound increases with pressure increasing and gas behavior is in good agreement with the classical theory. When Γ reaches 1, equation (2.9) shows that the speed of sound remains as a constant while pressure is increasing or decreasing, and pressure is a linear function of density only. When Γ is smaller than 1, the speed of sound turns to decrease with increasing pressure. Accompanying the change of the speed of sound, the gas starts to show some unconventional behavior. If Γ goes further below 0, equation (2.5) shows that isentropes in this region have negative curvature and the gas dynamic behaviors are totally different or even opposite to those based on classical theory. These unconventional behaviors will be discussed in later chapters.

Table 2.1: Gas behavior related to the sign and value of the fundamental derivative Γ

$\Gamma > 1$	$\left(\dfrac{\partial c}{\partial v}\right)_s < 0$	classical near ideal-gas behavior
$0 < \Gamma \leqslant 1$	$0 < \left(\dfrac{\partial c}{\partial v}\right)_s < \dfrac{c}{v}$	classical real-gas behavior
$\Gamma \leqslant 0$	$\left(\dfrac{\partial c}{\partial v}\right)_s > \dfrac{c}{v}$	non-classical behavior

2.3 Calculation of the Fundamental Derivative from the Equation of State

The four different expressions of the fundamental derivative Γ are listed below.

$$\Gamma = \frac{c^4}{2v^3}\left(\frac{\partial^2 v}{\partial p^2}\right)_s$$
$$\Gamma = \frac{v^3}{2c^2}\left(\frac{\partial^2 p}{\partial v^2}\right)_s$$
$$\Gamma = \frac{1}{c}\left(\frac{\partial \rho c}{\partial \rho}\right)_s = 1 - \frac{v}{c}\left(\frac{\partial c}{\partial v}\right)_s$$
$$\Gamma = 1 + \frac{c}{v}\left(\frac{\partial c}{\partial p}\right)_s$$

All of them are expressed in terms of derivative along an isentrope. By applying thermodynamic equations and Maxwell relation, Bethe[25] gave an alternative expression for Γ by using v and T as the independent thermodynamic state variables (see Appendix A)

$$\Gamma(T,v) = \frac{v^3}{2c^2}\left[\frac{\partial^2 p}{\partial v^2} - \frac{3T}{c_v}\frac{\partial p}{\partial T}\frac{\partial^2 p}{\partial T \partial v} + \left(\frac{T}{c_v}\frac{\partial p}{\partial T}\right)^2\left[\frac{3}{T}\frac{\partial c_v}{\partial v} + \frac{1}{T}\frac{\partial p}{\partial T}\left(1 - \frac{T}{c_v}\frac{\partial c_v}{\partial T}\right)\right]\right] \quad (2.10)$$

where $p = p(T,v), c_v(T,v) = \dfrac{\partial e(T,v)}{\partial T}$.

Equation (2.10) provides a convenient way to calculate the value of Γ by using the equation of state directly. For example, if substituting the ideal gas law and assuming constant specific heats, the equation of Γ can be simplified as

$$\Gamma = \frac{1}{2}\left(\frac{c_p}{c_v} + 1\right) = \frac{\gamma + 1}{2} \tag{2.11}$$

which gives the value of Γ for a perfect gas.

2.4 Thermodynamic properties of MDM

The regular gases usually do not have a negative fundamental derivative region, because negative Γ requires gases of high molecular complexity. Earlier researchers had doubts about the existence of the so-called BZT gas and the related non-classical gas behavior. Examples of BZT fluids have been identified for certain heavy hydrocarbons and some methylsiloxanes[26]. Some behaviors of BZT fluids have been studied extensively in recent years[27], focusing on the sonic shock and double-sonic shock. But so far there is not yet a complete set of theory to describe how each flow variable changes along the isentrope.

In the present work, a compound gas named Octamethyltrisiloxane (also called MDM) is chosen as the working fluid. It is an organosilicon compound with the formula $C_8H_{24}O_2Si_3$. Organometallics are useful reagents, catalysts, and precursor materials with applications in thin film deposition, industrial chemistry, pharmaceuticals, LED manufacturing, and others. The chemical structure [28] and some basic properties of Octamethyltrisiloxane are given in Table 2.2.

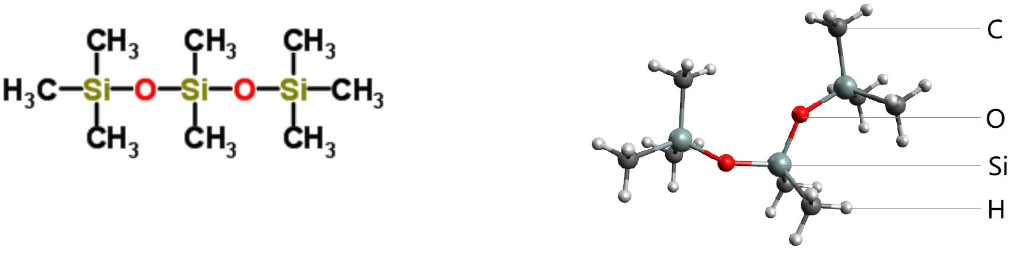

(a) 2D view

(b) 3D view

Figure 2.2: Chemical structure of $C_8H_{24}O_2Si_3$

Table 2.2: Properties of $C_8H_{24}O_2Si_3$

Gas	$C_8H_{24}O_2Si_3$
Molecular Weight	$M_g = 236.53146 \times 10^{-3}\ (kg/mol)$
Critical Pressure	$p_c = 1410045\ (Pa)$
Critical Temperature	$T_c = 564.09\ (K)$
Gas Constant	$R = 35.1516\ (J/(kg \cdot K))$
Degree of Freedom	$N = 57.96$
Specific Heat at constant volume	$c_v = N * R\ (J/(kg \cdot K))$
Constants in Van der Waals EoS	$a = \frac{27R^2T_c^2}{64p_c}\ (Pa \cdot m^6/kg^2)$
	$b = \frac{RT_c}{8p_c}\ (m^3/kg)$

The three significant regions of Γ are marked out in the $p - v$ plane by the $\Gamma = 0$ and $\Gamma = 1$ contour lines shown in Figure 2.3. There is a non-negligible region where the Γ is smaller than 0. Computation of this plot is based on the Van der Waals equation of state. Compared to a regular gas of positive fundamental derivative, this gas shows some non-classical properties near its critical point, which will be discussed later.

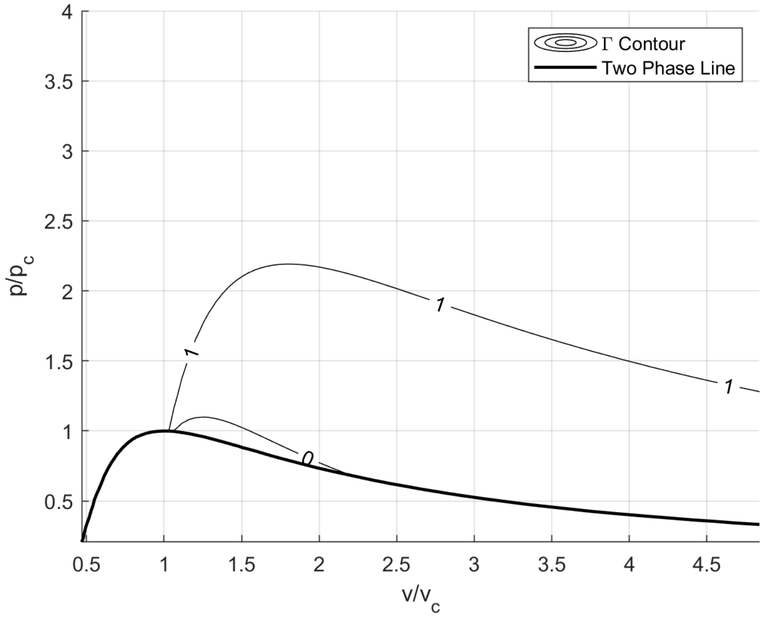

Figure 2.3: Contours of Γ in the p-v plane for MDM

Chapter 3

General Isentropic Flow Relations for Non-ideal Gas

The ideal gas assumption is widely used in gas dynamic analysis. An ideal gas is one that follows the ideal gas laws at all conditions of temperature and pressure. To do so, the gas would need to completely abide by the following assumptions:

- The gas molecules are so small that their volume is negligible compared with the volume occupied by the gas. Therefore, the molecule can be considered as a "point mass".
- The average distance between molecules is much larger than the characteristic length of the molecules, and the gas molecules are constantly moving in random directions with a distribution of speeds.
- There is neither attractive nor repulsive energy included throughout the collision of molecules. All collisions between gas molecules or the surroundings are elastic and all motions are frictionless. No energy is lost in collisions or in motion, or to say, the kinetic forces will remain unchanged in gas molecules due to the lack of intramolecular

energy.

The ideal gas law is just an idealization or approximation to the behavior of gases. At room temperature and pressure, real gases tend to behave very much like ideal gases. But when gas is near its critical point, forcing its molecules closer together as the space between the particles is diminished, the gas will behave less ideally. The unavailable volume for molecule motion as well as the attraction and repulsion forces between the molecules need to be taken into account. The ideal gas law does not work well under those conditions, which leads to the necessity of investigating the thermodynamics of real gas.

It is convenient to start the analysis of unconventional gas dynamics by studying the isentropic flow in a quasi-1D nozzle. Quasi-one-dimensional flow means that there are no transverse variations in the flow properties. So, the properties are only changing in the direction of the flow. Although the analysis may be regarded as an approximation to the flow in a nozzle, the equations and thus the results are exact for an inviscid flow through a streamtube or streamline in a three-dimensional flow field.

3.1 Speed of Sound

Consider an inviscid isentropic flow through a channel of cross-sectional area $A(x)$, where x represents the flow direction. The conservation of momentum is given as

$$\rho u du + dp = 0 \tag{3.1}$$

Since the flow is isentropic, Equation (2.9) gives $vdp = \dfrac{cdc}{\Gamma - 1}$. Substituting the above into

Equation (3.1) yields

$$udu + \frac{cdc}{\Gamma - 1} = 0 \tag{3.2}$$

In the ideal gas situation, we are familiar with the result that as a flow accelerates its temperature and sound speed decrease monotonically. Equation (3.2) re-states this result for the ideal gas but reveals the opposite behavior for a real gas with $\Gamma < 1$, as shown in Table 3.1. For a real gas with $\Gamma < 1$, the sound speed increases as the flow accelerates downstream.

Table 3.1: Speed of sound - Velocity relation related to Γ

Γ	Gas Behavior
$\Gamma > 1$	speed of sound decreases with u increasing
$\Gamma < 1$	speed of sound increases with u increasing

3.2 Isentropic Exponents

3.2.1 Definition of Real Isentropic Exponents

One is familiar with the simple and elegant thermodynamic and isentropic flow relations based on the ideal gas assumption. The familiar isentropic relations of an ideal gas are given below

$$pv^{\gamma} = constant \tag{3.3}$$

$$Tv^{\gamma-1} = constant \tag{3.4}$$

$$Tp^{\frac{1-\gamma}{\gamma}} = constant \tag{3.5}$$

where $\gamma = \dfrac{c_p}{c_v}$ is the ratio of specific heats.

The corresponding differential relations to Equations (3.3)-(3.5) are

$$\frac{dp}{p} = -\gamma \frac{dv}{v} \tag{3.6}$$

$$\frac{dT}{T} = -(\gamma - 1)\frac{dv}{v} \tag{3.7}$$

$$\frac{dp}{p} = \frac{\gamma}{\gamma - 1}\frac{dT}{T} \tag{3.8}$$

For a real gas, γ is no longer a constant and the above relations are in general invalid. In an attempt to retain the same simple exponential form, Kouremenos and Kakatsios[29] proposed the use of three different isentropic exponents corresponding to equation (3.6) - (3.8) for each pair formed out of the variables p, v, T, expressed as γ_{pv}, γ_{Tv} and γ_{pT}, respectively. Notice these exponents are not constants. They vary with the thermodynamic state. Therefore, they should be regarded as local exponents. For example, in the (p, v) plane the pressure-volume exponent γ_{pv} can be defined according to Equation (3.6) as

$$\left(\frac{dp}{dv}\right)_s = \gamma_{pv}\frac{p}{v} \tag{3.9}$$

Recall the expression of the entropy change in terms of pressure and specific volume

$$ds = \left(\frac{\partial s}{\partial p}\right)_v dp + \left(\frac{\partial s}{\partial v}\right)_p dv = 0 \tag{3.10}$$

Rearranging the partial derivatives yields

$$\left(\frac{dp}{dv}\right)_s = -\frac{\left(\frac{\partial s}{\partial v}\right)_p}{\left(\frac{\partial s}{\partial p}\right)_v} \tag{3.11}$$

The right hand side of equation (3.11) can be re-expressed using the Maxwell relations and the triple product rule

$$-\frac{\left(\frac{\partial s}{\partial v}\right)_p}{\left(\frac{\partial s}{\partial p}\right)_v} = \frac{\left(\frac{\partial p}{\partial T}\right)_s}{\left(\frac{\partial v}{\partial T}\right)_s} = \frac{\left(\frac{\partial p}{\partial s}\right)_T\left(\frac{\partial s}{\partial T}\right)_p}{\left(\frac{\partial v}{\partial s}\right)_T\left(\frac{\partial s}{\partial T}\right)_v} = -\frac{c_p}{c_v}\left(\frac{\partial T}{\partial v}\right)_p\left(\frac{\partial p}{\partial T}\right)_v = \frac{c_p}{c_v}\left(\frac{\partial p}{\partial v}\right)_T \tag{3.12}$$

where $c_p/T = \left(\frac{\partial s}{\partial T}\right)_p$ and $c_v/T = \left(\frac{\partial s}{\partial T}\right)_v$.

Combining Equations (3.9), (3.11) and (3.12), we obtain the pressure-volume exponent in terms of the state variables

$$\gamma_{pv} = -\frac{v}{p}\frac{c_p}{c_v}\left(\frac{\partial p}{\partial v}\right)_T \tag{3.13}$$

Similarly, the temperature-volume exponent can be defined in accordance with Equation (3.7), as derived from the temperature-volume relation along an isentrope, i.e,

$$\gamma_{Tv} = 1 - \frac{v}{T}\left(\frac{dT}{dv}\right)_s \tag{3.14}$$

Starting with defining the entropy as a function of temperature and specific volume $s = s(T, v)$, the derivatives are related as

$$\left(\frac{dT}{dv}\right)_s = -\frac{\left(\frac{\partial s}{\partial v}\right)_T}{\left(\frac{\partial s}{\partial T}\right)_v} \tag{3.15}$$

Following the same steps as previously for the pressure-volume exponent, we obtain the expression for the temperature-volume exponent

$$\gamma_{Tv} = 1 + \frac{v}{c_v}\left(\frac{\partial p}{\partial T}\right)_v \tag{3.16}$$

As in the cases of deriving the previous two isentropic exponents, the pressure-temperature exponent is defined from Equation (3.8) as

$$\frac{\gamma_{pT}}{\gamma_{pT}-1} = \frac{T}{p}\left(\frac{dp}{dT}\right)_s \tag{3.17}$$

We again express it in terms of only the equation of state. Note

$$\left(\frac{dp}{dT}\right)_s = -\frac{\left(\dfrac{\partial s}{\partial T}\right)_p}{\left(\dfrac{\partial s}{\partial p}\right)_T} \tag{3.18}$$

The final expression of the pressure-temperature exponent is given as

$$\gamma_{pT} = \frac{1}{1-\dfrac{p}{c_p}\left(\dfrac{\partial v}{\partial T}\right)_p} \tag{3.19}$$

Notice that the exponents as defined above are identical to γ for the ideal gas case. For a general real gas, they are different and non-constant. However, only two of the three are independent. Eliminating the partial derivatives, the relation between the three real isentropic exponents is

$$\frac{\gamma_{pv}}{\gamma_{Tv}-1} = \frac{\gamma_{pT}}{\gamma_{pT}-1} \tag{3.20}$$

3.2.2 Other Variables in Terms of Isentropic Exponents

By defining the three real isentropic exponents, other flow properties can be derived from them or be related to them, including entropy production, speed of sound and Mach number, etc.

Consider the entropy change as a function of temperature and specific volume

$$ds = \left(\frac{\partial s}{\partial T}\right)_v dT + \left(\frac{\partial s}{\partial v}\right)_T dv \tag{3.21}$$

Replacing the term $\left(\frac{\partial s}{\partial T}\right)_v$ by $\frac{c_v}{T}$ and substituting equation (3.16) into the second term on the right hand side in Equation (3.21) yields

$$ds = c_v \frac{dT}{T} + c_v(\gamma_{Tv} - 1)\frac{dv}{v} \tag{3.22}$$

The speed of sound can be derived as

$$c^2 = \left(\frac{\partial p}{\partial \rho}\right)_s = -v^2 \left(\frac{\partial p}{\partial v}\right)_s = \gamma_{pv} p v \tag{3.23}$$

and thus the Mach number is

$$M = \frac{u}{c} = \frac{u}{\sqrt{\gamma_{pv} p v}} \tag{3.24}$$

3.3 Stagnation Properties

In fluid dynamics, the total or stagnation properties of the fluid provide a convenient reference state of a fluid in motion. Looking into the original definition of total properties, the total pressure and total density are the pressure and density at the stagnation point when the fluid is brought to rest isentropically, and the total temperature is the temperature at the stagnation point when the fluid is brought to rest adiabatically (is automatically satisfied if the process is isentropic). At a stagnation point, the speed of the fluid is zero, and all of the kinetic energy has been converted to internal energy and is added to the local static enthalpy. Classical theory has already established the analytical expression of stagnation properties for a calorically perfect gas, which is

$$h_0 = c_p T_0 \tag{3.25}$$

$$p_0 = p \left[1 + \frac{\gamma - 1}{2} M^2\right]^{\frac{\gamma}{\gamma-1}} \tag{3.26}$$

$$T_0 = T \left[1 + \frac{\gamma - 1}{2} M^2\right] \tag{3.27}$$

$$\rho_0 = \rho \left[1 + \frac{\gamma - 1}{2} M^2\right]^{\frac{1}{\gamma-1}} \tag{3.28}$$

These familiar equations are no longer valid for real gases. To build up a theory of stagnation properties for real gases, the first step is to understand the change of isentropic exponents along the isentrope. Nederstigt [30] introduced the assumption of locally constant values for the isentropic exponents between isentropic states. For low subsonic flows, the kinetic energy contained in the flow is much smaller than the static enthalpy of the flow, leading to small changes in the isentropic state so that the isentropic exponents can be assumed to be constants along the stagnation process. But this assumption leads to an inaccurate evaluation of the values of stagnation properties. The differences between results by applying this assumption and the results by using the original definition (bringing the fluid to rest isentropically and doing the integral directly for every small thermodynamic state change) will be shown later.

To derive the total properties in terms of isentropic exponents, we start with the total enthalpy conservation law

$$\begin{aligned} h_0 &= h + \frac{u^2}{2} = constant \\ \Delta h &= \frac{u^2}{2} \end{aligned} \tag{3.29}$$

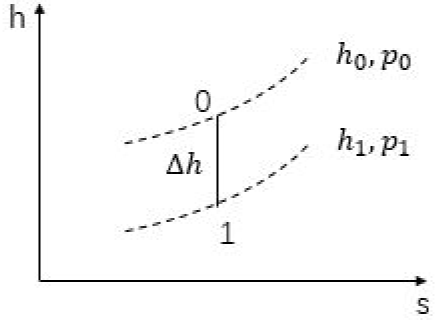

Figure 3.1: Sketch of total enthalpy definition

The expression of enthalpy change is also given by thermodynamic relation

$$dh = Tds + vdp \tag{3.30}$$

In an isentropic process, $ds = 0$. Thus, the enthalpy change from state 1 to state 2 is

$$\begin{aligned} h_2 - h_1 = \int_1^2 vdp = \int_1^2 v_1 \left(\frac{p_1}{p}\right)^{\frac{1}{\gamma_{pv}}} dp = v_1 p_1 \left(\frac{\gamma_{pv}}{\gamma_{pv}-1}\right)\left[\left(\frac{p_2}{p_1}\right)^{\frac{\gamma_{pv}-1}{\gamma_{pv}}} - 1\right] \\ \Delta h = vp\left(\frac{\gamma_{pv}}{\gamma_{pv}-1}\right)\left[\left(\frac{p_0}{p}\right)^{\frac{\gamma_{pv}-1}{\gamma_{pv}}} - 1\right] \end{aligned} \tag{3.31}$$

Here the assumption of locally constant value of γ_{pv} is applied. In other words, equation (3.31) is only valid for small thermodynamic state changes, and the value of γ_{pv} is updated in each step. Both Equations (3.29) and (3.31) describes the enthalpy change through an isentropic process. Equating Equations. (3.29) and (3.31) gives

$$\frac{p_0}{p} = \left[1 + \frac{\gamma_{pv}-1}{2}M^2\right]^{\frac{\gamma_{pv}}{\gamma_{pv}-1}} \tag{3.32}$$

The total pressure for real gas flow in terms of real isentropic exponents is given as

$$p_0 = p\left[1 + \frac{\gamma_{pv} - 1}{2} M^2\right]^{\frac{\gamma_{pv}}{\gamma_{pv}-1}} \tag{3.33}$$

Derived by the same procedure, the total temperature and total density in terms of real isentropic exponents are

$$T_0 = T\left[1 + \frac{\gamma_{pv} - 1}{2} M^2\right]^{\frac{\gamma_{Tv}-1}{\gamma_{pv}-1}} \tag{3.34}$$

$$\rho_0 = \rho\left[1 + \frac{\gamma_{pv} - 1}{2} M^2\right]^{\frac{1}{\gamma_{pv}-1}} \tag{3.35}$$

The form of these expressions of total variables is similar to those have been commonly used for ideal gas computation. To compare with the ideal gas law, Figures 3.2, 3.3 and 3.4 plot the pressure, temperature and density computed by both methods. The figures show that for very low Mach number and very high Mach number, the differences are negligible. Recalling the assumptions made in previous sections, the real gas assumption indicates that more internal energy is contained in the flow, and the locally constant values for the isentropic exponents assume that the kinetic energy contained in the flow is much smaller than the static enthalpy of the flow. These two assumptions are ambivalent especially when Mach number is high, leading to the inaccurate evaluation of the values of stagnation properties by using Equations (3.33), (3.34), and (3.35).

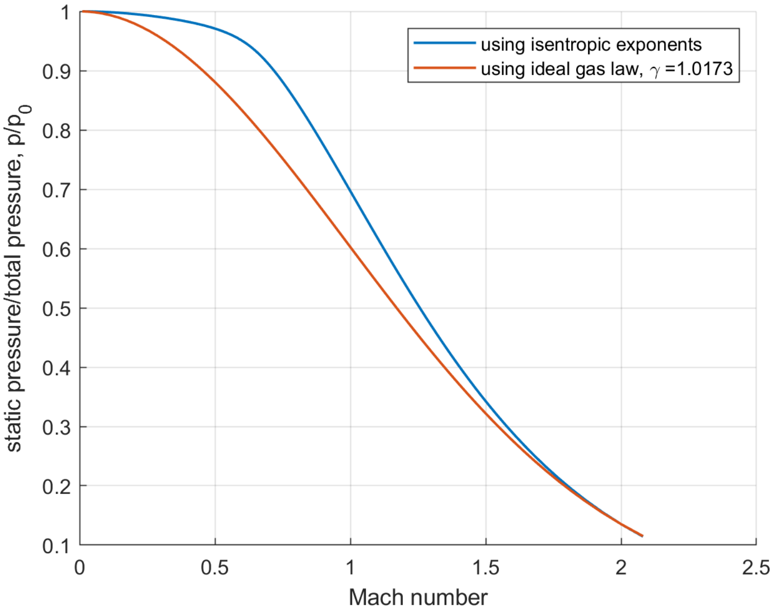

Figure 3.2: Comparison of pressure calculated by different methods (MDM gas)

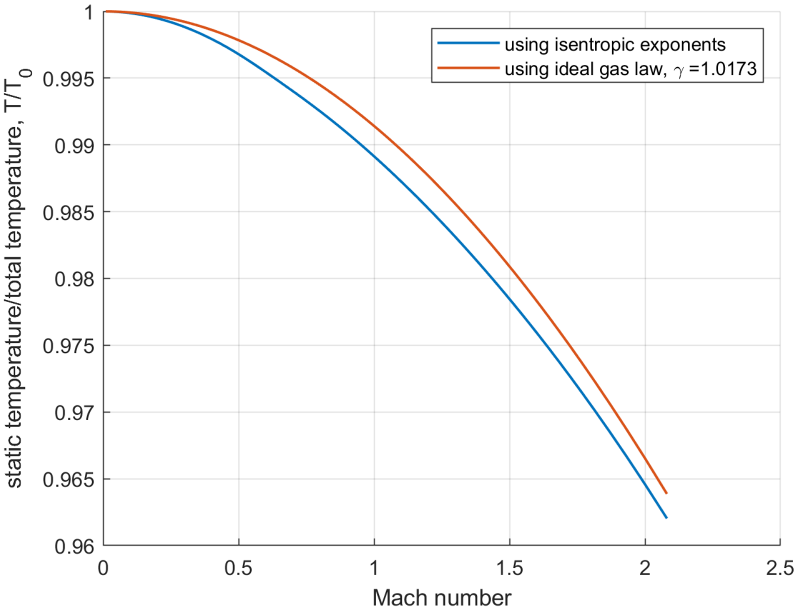

Figure 3.3: Comparison of temperature calculated by different methods (MDM gas)

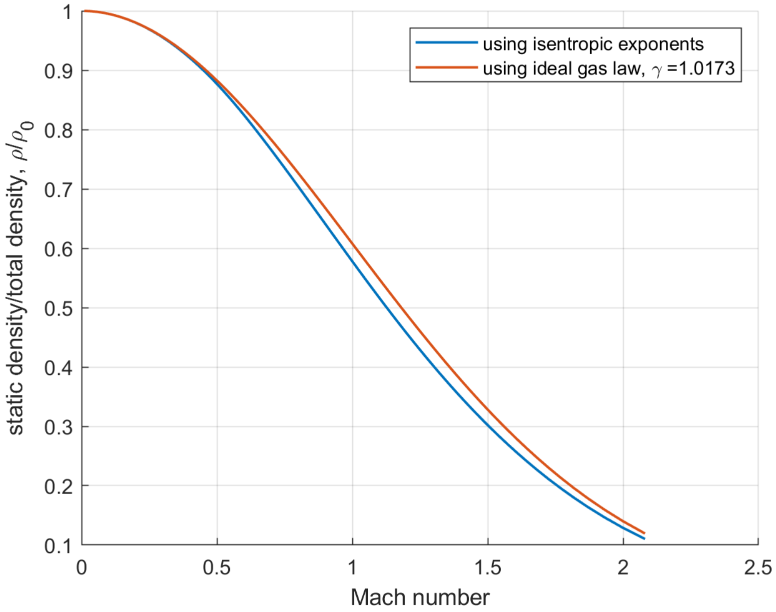

Figure 3.4: Comparison of density calculated by different methods (MDM gas)

Besides the differences with ideal gas equations, we will also demonstrate that these expressions for total properties with isentropic exponents are not accurate, especially when the Mach number is high. As mentioned before, the computational results by using equation (3.33), (3.34) and (3.35) are compared with the results by applying the original definition of total properties (integrate the variables from any velocity u to rest isentropically). Figure 3.5 and 3.6 show the comparison of the total properties of an isentropic flow of MDM computed by different methods. The upstream condition is $p_{in} = 1.1p_c$, $v_{in} = 1.0v_c$, $M_{in} = 0.5$ and the flow ends at $p_b = 0.5p_c$. It can be seen that the total pressure and total enthalpy are conserved by using the original definition, whereas the isentropic exponents' expressions cannot agree with the conservation laws. As the Mach number increases from 0.5 to 1.3, the errors in both p_0 and h_0 exceed more than 10%.

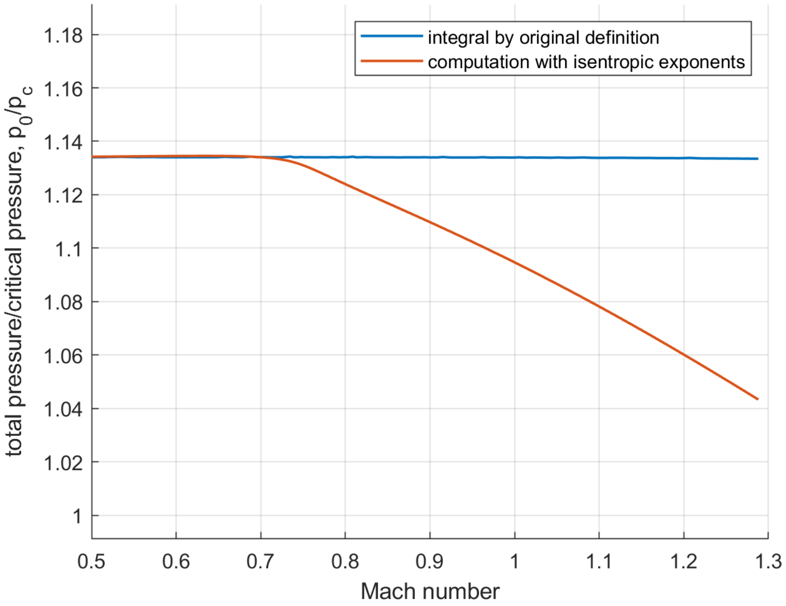

Figure 3.5: Comparison of total pressure calculated by different methods

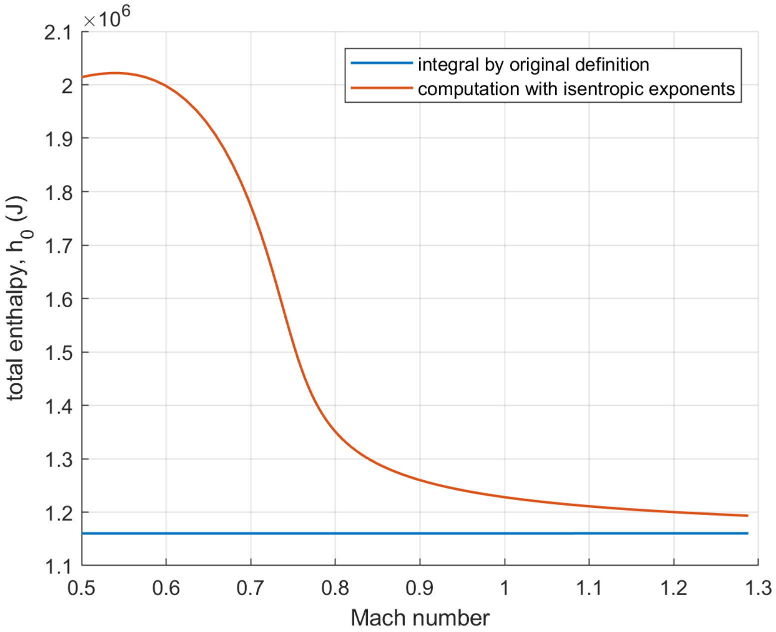

Figure 3.6: Comparison of total enthalpy change calculated by different methods

Figures 3.7 and 3.8 present results for the same isentropic process outlined above. Figure 3.7 shows the variation of different exponents γ_{pv}, γ_{Tv} and γ_{pT}, together with the value of c_p/c_v (c_p here is calculated by using Van der Waals equation of state) and $(c_v + R)/c_v$ (the γ defined in perfect gas law). Usually, the values of these exponents are larger than 1. But within the non-classical region, the isentrope is a convex curve in the p-v diagram (as shown in Figure 2.1), leading to the value of γ_{pv} much smaller than 1. Figure 3.8 is the isentrope plotted on a logarithmic scale, compared with an isentrope passing through the same thermodynamic state but calculated with ideal gas assumption. As mentioned before, the real isentropic exponents only keep constants locally and vary with the thermodynamic state variables along the isentrope.

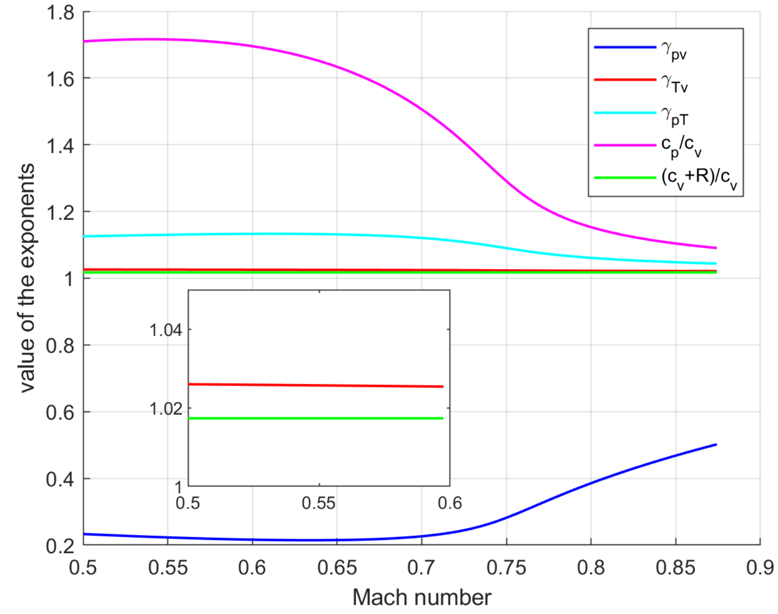

Figure 3.7: Comparison of the variation of different exponents

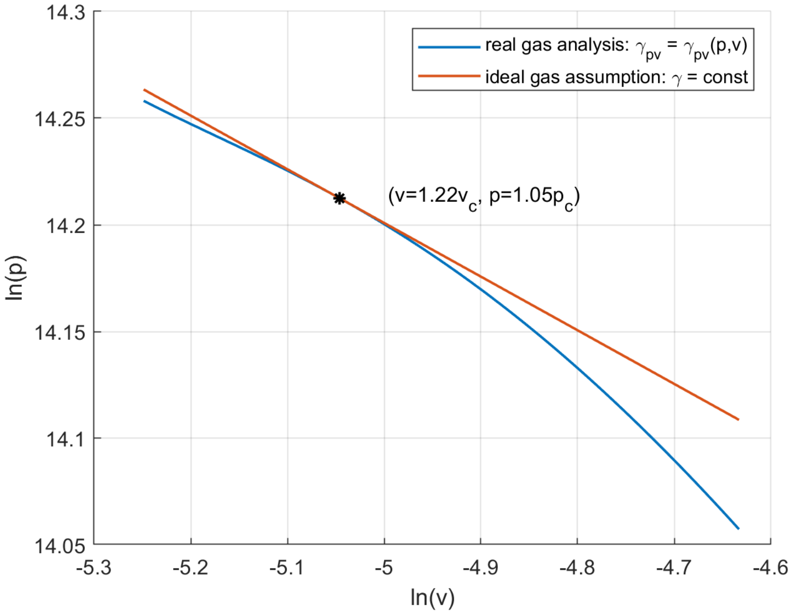

Figure 3.8: Comparison of the real isentropic exponent γ_{pv} with ideal gas γ

3.4 Specific Heat Function and Enthalpy

For an ideal gas, the specific heat capacities can be elegantly related to the universal gas constant

$$c_p - c_v = R$$

They can also be expressed as a function of the adiabatic coefficient and the universal gas constant

$$c_p = \frac{\gamma R}{\gamma - 1} \quad \text{and} \quad c_v = \frac{R}{\gamma - 1}$$

Enthalpy comprises a system's internal energy. It is defined as a state function that depends on pressure and temperature. By applying the ideal gas law, enthalpy can be simplified as a function of temperature only.

$$dh = c_p(T)dT \quad , \quad h = h(T)$$

Actually, this expression is under the assumption of a thermodynamic perfect gas. To be more restricted, the calorically perfect gas assume the heat capacity to be constant, which is, $h = c_pT$.

The relation between the specific heat capacities for a real gas is given as

$$c_p - c_v = T\left(\frac{\partial v}{\partial T}\right)_p \left(\frac{\partial p}{\partial T}\right)_v \tag{3.36}$$

And the differential form of enthalpy change can be written as

$$dh = \left(\frac{\partial h}{\partial T}\right)_p dT + \left(\frac{\partial h}{\partial p}\right)_T dp \tag{3.37}$$

Recall the enthalpy equation derived from Gibbs relation

$$dh = vdp + Tds \tag{3.38}$$

Divide by dp on both sides of equation (3.38)

$$\left(\frac{\partial h}{\partial p}\right)_T = v + T\left(\frac{\partial s}{\partial p}\right)_T \tag{3.39}$$

The second term on RHS can be rewritten by Using Maxwell relation

$$\left(\frac{\partial s}{\partial p}\right)_T = -\left(\frac{\partial v}{\partial T}\right)_p \tag{3.40}$$

Then equation (3.39) becomes

$$\left(\frac{\partial h}{\partial p}\right)_T = v - T\left(\frac{\partial v}{\partial T}\right)_p \tag{3.41}$$

Substitute equation (3.41) into equation (3.37), the general form for calculating the enthalpy of a non-ideal gas is given as

$$dh = c_p dT + \left[v - T\left(\frac{\partial v}{\partial T}\right)_p\right] dp \tag{3.42}$$

Different gas models and equations of state can be applied to this equation. For example, the present work has selected the Van der Waals equation of state for numerical computation. The equation of state is given as

$$p = \frac{RT}{v-b} - \frac{a}{v^2} \tag{3.43}$$

Take partial derivative of equation (3.43)

$$\left(\frac{\partial T}{\partial p}\right)_v = v - b \tag{3.44}$$

$$\left(\frac{\partial p}{\partial v}\right)_T = \frac{-RT}{(v-b)^2} + \frac{2a}{v^3} \tag{3.45}$$

Recall the triple product rule of partial derivative

$$\left(\frac{\partial v}{\partial T}\right)_p \left(\frac{\partial T}{\partial p}\right)_v \left(\frac{\partial p}{\partial v}\right)_T = -1 \tag{3.46}$$

$\left(\frac{\partial v}{\partial T}\right)_p$ then can be expressed as

$$\left(\frac{\partial v}{\partial T}\right)_p = \frac{v^3(v-b)}{RTv^3 - 2a(v-b)^2} \tag{3.47}$$

Substituting equation (3.47) into equation (3.42), the differential form of enthalpy equation for Van der Waals gas is

$$dh = c_p dT + \left[v - \frac{Tv^3(v-b)}{RTv^3 - 2a(v-b)^2}\right] dp \tag{3.48}$$

3.5 Mach number - Velocity Relation

Recall equation (3.2)

$$udu + \frac{cdc}{\Gamma - 1} = 0$$

Let $M = u/c$, substitute M into the equation above and simplify the result.

$$\begin{aligned} dM &= \frac{1}{c}du - \frac{u}{c^2}dc \\ \frac{dc}{c} &= \frac{du}{u} - \frac{dM}{M} \\ udu &+ \frac{c^2}{\Gamma - 1}\left(\frac{du}{u} - \frac{dM}{M}\right) = 0 \end{aligned}$$

Then, the relation between velocity and Mach number is

$$\frac{du}{u} = \frac{1}{1 + (\Gamma - 1)M^2}\frac{dM}{M} \tag{3.49}$$

Equation (3.49) shows how the Mach number would be changed with velocity. For any classical gas with $\Gamma > 1$, Mach number always increases with the velocity monotonically. But for a non-classical gas when Γ goes below 1, the change of Mach number would be depending on the sign of the term $1 + (\Gamma - 1)M^2$. When $M^2 < \frac{1}{1 - \Gamma}$, Mach number still increases with velocity like how it behaves in the classical gas case. Otherwise, if $M^2 > \frac{1}{1 - \Gamma}$, Mach number will decrease with velocity and therefore show some non-classical properties.

Table 3.2: Mach - Velocity relation related to Γ

Γ	Gas Behavior
$\Gamma > 1$	M increases monotonically with u
$\Gamma < 1$	M increases with u only for $M^2 < \frac{1}{1 - \Gamma}$

3.6 Mach number - Area Relation

Classical theory has established a complete system for quasi-1D nozzle flow. Consider a quasi-1D isentropic flow, the velocity-area relation is given as

$$\frac{1}{u}\frac{du}{dx} = \frac{M^2-1}{A}\frac{dA}{dx} \tag{3.50}$$

Substituting equation (3.50) into equation (3.49), the relation between Mach number and area change is

$$\frac{1}{M}\frac{dM}{dx} = \frac{1+(\Gamma-1)M^2}{M^2-1}\frac{1}{A}\frac{dA}{dx} \tag{3.51}$$

Equation (3.51) states that the transition between subsonic and supersonic flow only occurs when $\frac{dA}{dx} = 0$, and how the Mach number changes regarding to area ratio is related to the sign of $(1+(\Gamma-1)M^2)/(M^2-1)$. Conventionally, along with the increasing cross-sectional area ratio, the Mach number increases in a supersonic flow and decreases in a subsonic flow. But for non-classical gas cases, there are some different gas behaviors shown below.

Figure 3.9 shows that the Mach number - Area relation is behaving in the opposite way with the conventional theory when $M^2 > \frac{1}{1-\Gamma}$. Along with the increasing cross-sectional area ratio, the Mach number decreases in a supersonic flow and increases in a subsonic flow. To investigate the flow properties at the transonic point, the second-order derivative with respect to area ratio change needs to be derived from equation (3.51). To avoid the

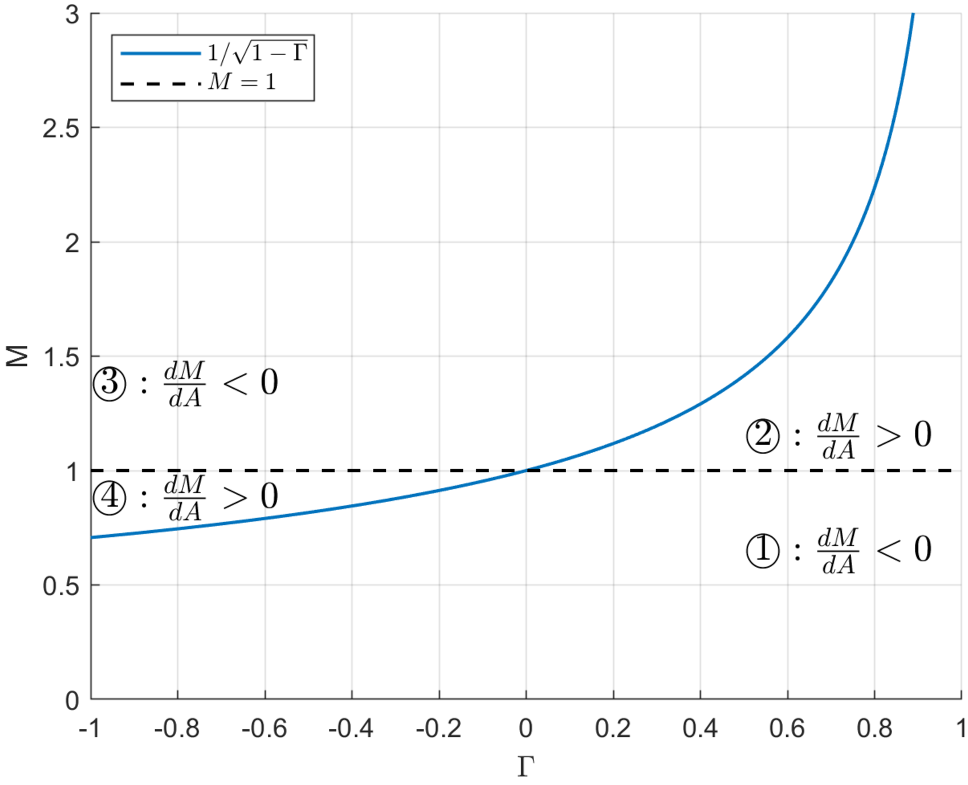

Figure 3.9: Mach number - Area relation related to Γ (for $\Gamma < 1$)

singularity value at transonic point $M = 1$, apply $L'Hospital's$ rule to equation (3.51)

$$\lim_{M\to1}\frac{dM}{dx} = \lim_{M\to1}\frac{\frac{d}{dx}\left[\left(1+(\Gamma-1)M^2\right)\frac{M}{A}\frac{dA}{dx}\right]}{\frac{d}{dx}\left[M^2-1\right]} \tag{3.52}$$

When $M \to 1$, $\dfrac{dA}{dx} \to 0$, so

$$\lim_{M\to1}\frac{dM}{dx} = \lim_{M\to1}\frac{1+(\Gamma-1)M^2}{2A\frac{dM}{dx}}\frac{d^2A}{dx^2} = \frac{\Gamma}{2A\frac{dM}{dx}}\frac{d^2A}{dx^2} \tag{3.53}$$

Rearrange the equation

$$\left(\frac{dM}{dx}\right)^2 = \frac{\Gamma}{2A}\frac{d^2A}{dx^2} \tag{3.54}$$

The LHS of equation (3.54) is always non-negative. So for gases with Γ greater than 0, The sonic point has the minimum cross-sectional area. However, when Γ goes smaller than 0, the cross-sectional area will have the maximum value at the sonic point. Instead of the classical convergent-divergent nozzle, here a divergent-convergent nozzle will be needed for non-classical gas transonic flow.

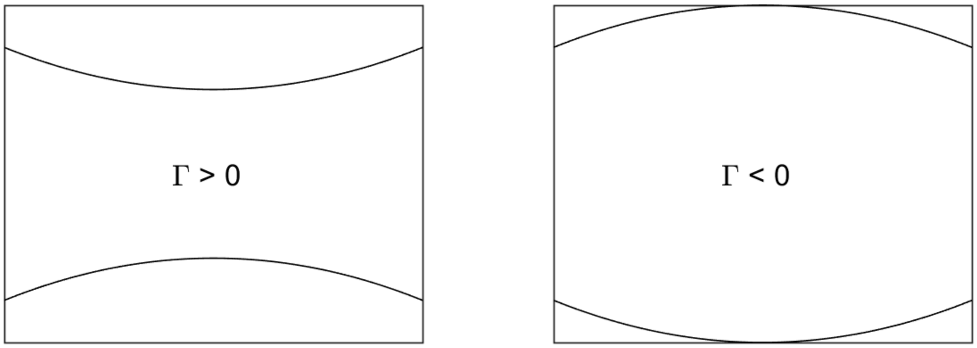

Figure 3.10: Transonic nozzle related to Γ

3.7 Differential Form of Conservation Laws

As discussed before, quasi-one-dimensional (Q1D) flow means that the flow properties change only in the direction of the flow and there are no transverse variations in the flow properties. In practical terms, a necessary (but not sufficient) condition for using the Q1D relations is that the channel cross-sectional area has gradual variations. This simplification is quite helpful and leads us to some interesting results.

Consider flow through a channel in which the flow direction is taken as x and has cross-sectional area $A(x)$. A mono-component, single-phase fluid flows isentropically through this channel. The conservation equations of mass, momentum, and energy are:

$$\begin{cases} \dfrac{d\rho}{\rho} + \dfrac{du}{u} + \dfrac{dA}{A} = 0 \\ \rho u du + dp = 0 \\ dh + u du = 0 \end{cases} \tag{3.55}$$

Equation (3.55) is the general form of conservation laws for isentropic Q1D flow. All the analyses for unconventional gas behavior in the present work are based on these equations. Rewriting equation (3.55) with expressions from former sections gives the following:
Momentum conservation:

$$\rho u du + dp = 0 \tag{3.56}$$

$$\rho u du + \left(\frac{\partial p}{\partial \rho}\right)_T d\rho + \left(\frac{\partial p}{\partial T}\right)_\rho dT = 0 \tag{3.57}$$

Energy conservation:

$$dh + u du = 0 \tag{3.58}$$

$$c_p dT + \left[v - T\left(\frac{\partial v}{\partial T}\right)_p\right] dp + u du = 0 \tag{3.59}$$

In practical conditions, the upstream and the downstream pressure of the channel will be given in most cases. To keep consistency with that, here the pressure difference is selected as the independent variable and all the other variables will be written in terms of dp.
First of all, the velocity difference can be derived from equation (3.56) directly

$$\frac{du}{dp} = -\frac{1}{\rho u} \tag{3.60}$$

The temperature difference regarding pressure is then given by equation (3.59)

$$\frac{dT}{dp} = \frac{T}{c_p}\left(\frac{\partial v}{\partial T}\right)_p \tag{3.61}$$

Once the temperature equation is obtained, substitute it into the following expression of dp

$$dp = \left(\frac{\partial p}{\partial \rho}\right)_T d\rho + \left(\frac{\partial p}{\partial T}\right)_\rho dT \tag{3.62}$$

which leads to the expression of density change with pressure

$$\frac{d\rho}{dp} = \frac{1 - \frac{T}{c_p}\left(\frac{\partial p}{\partial T}\right)_\rho \left(\frac{\partial v}{\partial T}\right)_p}{\left(\frac{\partial p}{\partial \rho}\right)_T} \tag{3.63}$$

So far the ordinary differential equation system for quasi-1D nozzle flow calculation is obtained:

$$\begin{cases} \dfrac{du}{dp} = -\dfrac{1}{\rho u} \\ \dfrac{dT}{dp} = \dfrac{T}{c_p}\left(\dfrac{\partial v}{\partial T}\right)_p \\ \dfrac{d\rho}{dp} = \dfrac{1 - \dfrac{T}{c_p}\left(\dfrac{\partial p}{\partial T}\right)_\rho \left(\dfrac{\partial v}{\partial T}\right)_p}{\left(\dfrac{\partial p}{\partial \rho}\right)_T} \end{cases} \tag{3.64}$$

To determine the local Mach number at each point, recall the Mach number-velocity relation, equation (3.49)

$$\frac{du}{u} = \frac{1}{1 + (\Gamma - 1)M^2}\frac{dM}{M}$$

The Mach number variation versus pressure is obtained by combining equation (3.49) with equation (3.60), which gives

$$\frac{dM}{dp} = -M(1 + (\Gamma - 1)M^2)\frac{1}{\rho u^2} \tag{3.65}$$

Chapter 4

Non-classical Behavior of a BZT Gas in Isentropic Quasi-1D Flow

To show the differences between conventional and unconventional gas behavior more clearly, several cases were run on our in-house code. The gas MDM introduced in Chapter 2 is selected as working fluid in the computation. There are some particular sections within the nozzle that the negative fundamental derivative condition could be achieved. Therefore, the unconventional gas behaviors are able to be observed. The theoretical relation discussed in previous chapters could be proved.

Section 4.1 briefly introduces the Van der Waals gas model and the derivative relations for the gas used in the present work. Section 4.2 and section 4.3 are isentropic cases started from the same point in the p-v diagram (same pressure and density) but with different upstream velocity, one in the subsonic area and the other one in the supersonic area. The inlet point was chosen to be as close to the critical point as it could be. In this way, the isentropic process we created will have a segment that across the negative fundamental derivative region and then stay in the $\Gamma < 1$ region until the nozzle outlet. The first subsonic case started at point $p_{in} = 1.1p_c, v_{in} = 0.8v_c$ with $M = 0.5$. The supersonic case started at $p_{in} = 1.1p_c, v_{in} = 0.8v_c$ with $M = 3$. Both of them have shown some interesting results which are opposite with the conventional behavior. To compare the differences between real gas results and ideal-gas results, two flows started from the same upstream condition but calculated by ideal-gas law are also shown.

4.1 Van der Waals Gas Relations

Equation (2.10) has shown the method to calculate the value of the fundamental derivative from the equation of state. Real gas equations of state like the Van der Waals equation or Soave-Redlich-Kwong equation are commonly used in researches. The present work has selected Van der Waals equation of state for computation, as it was the first, simplest and best-known equation of state to account for the real gas effects. Be more specific, it has accounted for inter-molecular attraction and the volume that a real gas molecule takes up. Due to the statistical nature of thermodynamic properties, the Van der Waals equation served as the earliest connection between the macroscopic behavior of the fluid and the microscopic interaction of molecules.

From previous chapters and sections, the equations needed for numerical computation are summarized here in table 4.1. All the equations are in differential form.

Table 4.1: Quasi-1D isentropic flow equations for non-conventional gas

Flow Variable	Calculation Formula
pressure	dp is taken as the independent variable
density	$\dfrac{d\rho}{dp} = \dfrac{1 - \dfrac{T}{c_p}\left(\dfrac{\partial p}{\partial T}\right)_\rho \left(\dfrac{\partial v}{\partial T}\right)_p}{\left(\dfrac{\partial p}{\partial \rho}\right)_T}$
temperature	$\dfrac{dT}{dp} = \dfrac{T}{c_p}\left(\dfrac{\partial v}{\partial T}\right)_p$
velocity	$\dfrac{du}{dp} = -\dfrac{1}{\rho u}$
cross-sectional area	$\dfrac{dA}{dp} = A\left(\dfrac{1}{\rho u^2} - \dfrac{\left[1 - \dfrac{T}{c_p}\left(\dfrac{\partial p}{\partial T}\right)_\rho \left(\dfrac{\partial v}{\partial T}\right)_p\right]}{\rho \left(\dfrac{\partial p}{\partial \rho}\right)_T}\right)$
Mach number	$\dfrac{dM}{dp} = -M(1 + (\Gamma - 1)M^2)\dfrac{1}{\rho u^2}$
Enthalpy	$dh = c_p dT + \left[v - T\left(\dfrac{\partial v}{\partial T}\right)_p\right] dp$
Specific Heat	$c_p - c_v = T\left(\dfrac{\partial v}{\partial T}\right)_p \left(\dfrac{\partial p}{\partial T}\right)_v$
Fundamental Derivative	$\Gamma(T, v) = \dfrac{v^3}{2c^2}\left[\dfrac{\partial^2 p}{\partial v^2} - \dfrac{3T}{c_v}\dfrac{\partial p}{\partial T}\dfrac{\partial^2 p}{\partial T \partial v} + \left(\dfrac{T}{c_v}\dfrac{\partial p}{\partial T}\right)^2 \left[3\dfrac{\partial^2 p}{\partial T^2} + \dfrac{1}{T}\dfrac{\partial p}{\partial T}\left(1 - \dfrac{T}{c_v}\dfrac{\partial p}{\partial T}\right)\right]\right]$

The solver in our in-house code is integrating the ODEs directly by using Table 4.1, with a uniform pressure change of $dp = 10^{-4} p_c$ between each interval. Vieta's formulas[31] are used to solve the EoS defined in Equation (4.1). Some expressions used in the code are given below in Table 4.2, principally are first-order and second-order derivatives from Van der Waals gas model. These expressions are mathematically simple, but they nevertheless adequately predict and explain the non-conventional gas behavior near the critical point.

Table 4.2: Relations from Van der Waals gas model

Flow Variable	Calculation Formula
Equation of State	$p = \frac{\rho R T}{1 - b\rho} - a\rho^2$
$\left(\frac{\partial p}{\partial T}\right)_v$	$\frac{R\rho}{1 - b\rho}$
$\left(\frac{\partial^2 p}{\partial T^2}\right)_v$	0
$\left(\frac{\partial p}{\partial \rho}\right)_T$	$\frac{RT}{(1 - b\rho)^2} - 2a\rho$
$\left(\frac{\partial p}{\partial v}\right)_T$	$-\frac{RT}{(v - b)^2} + \frac{2a}{v^3}$
$\left(\frac{\partial^2 p}{\partial v^2}\right)_T$	$\frac{2RT}{(v - b)^3} - \frac{6a}{v^4}$
$\left(\frac{\partial^2 p}{\partial T \partial v}\right)_T$	$-\frac{RT}{(v - b)^2}$
$\left(\frac{\partial v}{\partial T}\right)_p$	$-\frac{\left(\frac{\partial p}{\partial T}\right)_v}{\left(\frac{\partial p}{\partial v}\right)_T}$
Specific Heat	$c_p = c_v\left(1 - \frac{T}{c_v}\frac{R^2}{2a\rho(1 - b\rho)^2 - RT}\right)$
Speed of Sound	$c = \sqrt{v^2(\frac{RT}{(v - b)^2} - \frac{2a}{v^3} + \frac{T}{c_v}\frac{R}{(v - b))^2}}$
Enthalpy	$h = c_v T - \frac{a}{v} + pv$

Furthermore, rewrite the Van der Waals EoS in polynomial form

$$Z^3 - (1 + B)Z^2 + AZ - AB = 0 \tag{4.1}$$

where

$$Z = \frac{pv}{RT}, \qquad A = \frac{pa}{(RT)^2}, \qquad B = \frac{pb}{RT}$$

Here the coefficients A and B are non-dimensional parameters related to intermolecular attraction and repulsion, respectively. For a perfect gas, $A = B = 0$. The value of these coefficients can reflect how far a real gas deviates from the ideal-gas behavior.

4.2 Isentropic Flow with Subsonic Inlet Condition

Consider a nozzle with an undetermined cross-sectional area. The pressure profile along the flow direction is given as a parabolic function to show more evidently the non-classical behavior of the cross-sectional area ratio distribution. This isentropic process was plotted in the p-v diagram together with the two-phase line and fundamental derivative contours, as shown in Figure 4.1. It can be seen that this isentrope is chosen to be as close to the saturation line and the critical point as possible. Hence, there will be a longer segment in the negative fundamental derivative region.

The fundamental derivative is a function of pressure and specific volume only. So, it can be calculated before solving the ODE system. Figure 4.2 has shown the distribution of fundamental derivative along the static pressure. Γ is greater than 1 at the inlet point ($p/p_c = 1.1$) and drops rapidly when the pressure starts to decrease. This drop happens

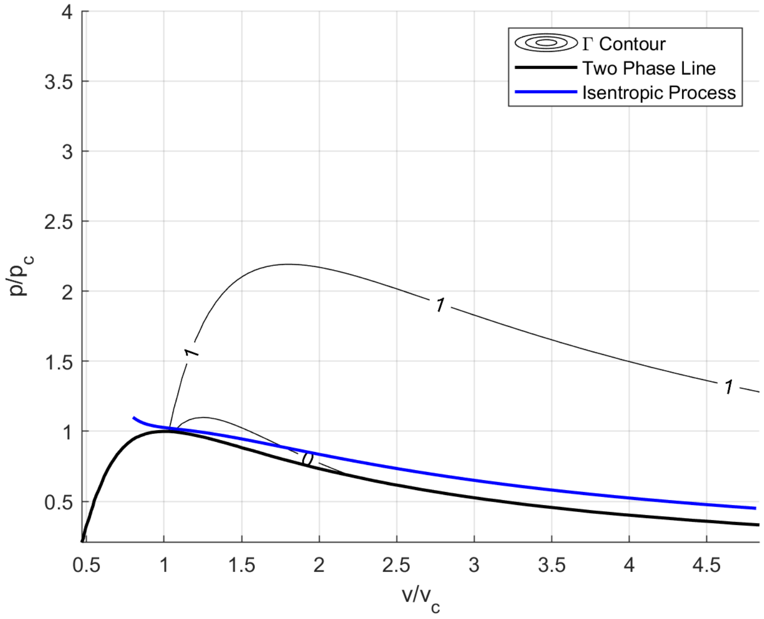

Figure 4.1: Case 1: $p_{in} = 1.1p_c, M_{in} = 0.5, v_{in} = 0.8v_c$

close to the critical point in the p-v diagram where the isentrope goes across multiple Γ contours. Away from the critical point, Γ goes less than 1 and still further away, it becomes less than 0. Then, it achieves its minimum value when the pressure equals the critical pressure of the gas and turns back to increase gradually. Apparently, Γ keeps staying in the $\Gamma < 1$ region until the nozzle outlet. Γ will eventually exceed 1 if the gas is going to be expanded to very low pressure. Based on our computation results, it requires the outlet pressure to be hundreds of times smaller than the inlet pressure.

Figure 4.3 gives the variation of non-dimensional variables A and B from equation (4.1). As mentioned, the isentrope is chosen to keep close to the critical point, and therefore the gas will behave least ideally. The values of A and B can show the nonideality of the gas behavior.

Figures 4.4a and 4.4b present the difference between the cross-sectional area ratio (A/A_{min}) by using ideal-gas law and Van der Waals model. Figures 4.4c and 4.4d plot the corresponding Mach number distribution. From Figures 4.4a and 4.4c it can be found that under the ideal-

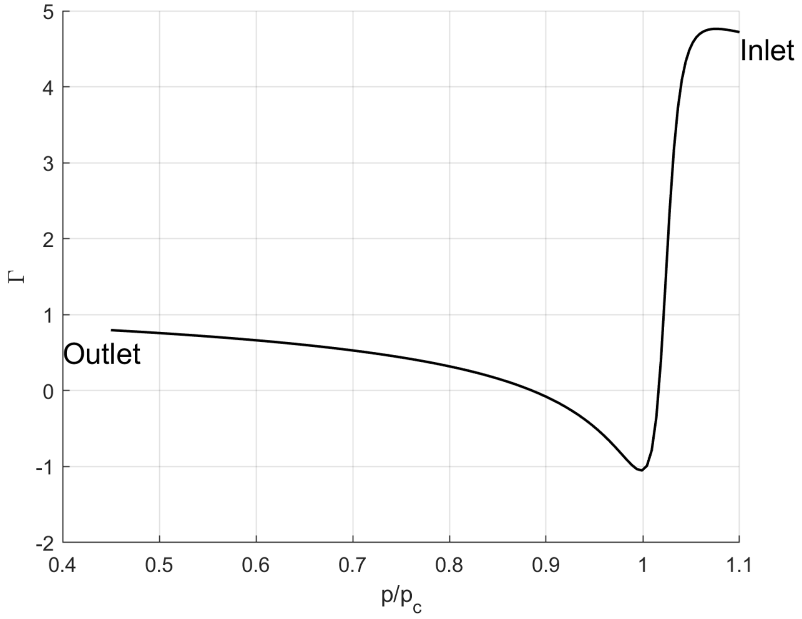

Figure 4.2: Fundamental derivative distribution(Case 1)

gas analysis, a convergent-divergent nozzle is needed for a transonic flow, in other words, the nozzle needs a 'throat' to achieve the sonic condition. The Mach number is a monotonic function of velocity. On the contrary, non-classical theory tells a different story. The 'throat' is no longer necessary for the sonic point, instead there is a locally maximum area when $M = 1$. Going back to Figure 3.9, when the Mach number falls into region 3 and region 4, the Mach number - Area relation will be opposite with the one from ideal-gas theory. Also when the Mach number exceeds 1, it is not a monotonic function of velocity anymore. Recall equation (3.49)

$$\frac{du}{u} = \frac{1}{1 + (\Gamma - 1)M^2} \frac{dM}{M}$$

This equation states that the Mach number increases monotonically with u when $\Gamma > 1$ and increases with u only for $M^2 < \dfrac{1}{1-\Gamma}$ when $\Gamma < 1$ (region 1 and region 2 in Figure 3.9). Figure 4.4d clearly shows that there is an area where Mach number is decreasing with velocity increasing (M falls into region 3 and region 4 in Figure 3.9), around $p/p_c = 0.9$ to

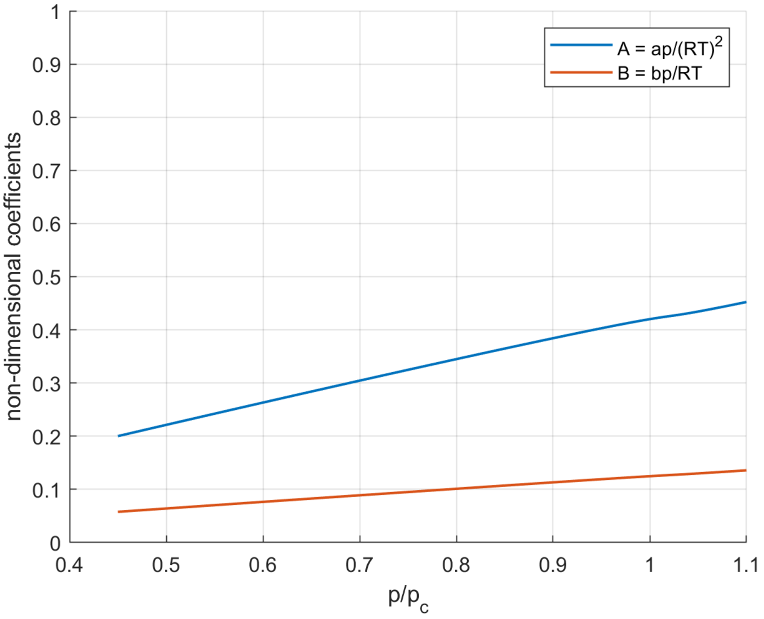

Figure 4.3: Variation of non-dimensional variables A and B (Case 1)

$p/p_c = 1.02$. Within this range, the fundamental derivative is decreasing rapidly while the Mach number doesn't change too much, so M^2 turns to be larger than $\dfrac{1}{1-\Gamma}$.

Figure 4.4b shows the relationship between the curvature of cross-sectional area change and the fundamental derivative, as what has been discussed in equation (3.54).

$$\left(\frac{dM}{dx}\right)^2 = \frac{\Gamma}{2A}\frac{d^2A}{dx^2}$$

The curvature of the cross-sectional area change A depends on the sign of Γ directly. When Γ is less than zero, the area change turns to be a convex function instead of a concave function.

Look at Figure 4.4b and Figure 4.4d, there are three sonic points in total. The first one and third one have fallen into $\Gamma > 0$ area which leads to the classical convergent-divergent part of the nozzle. The sonic point in the middle is the interesting one. At this point, Γ is

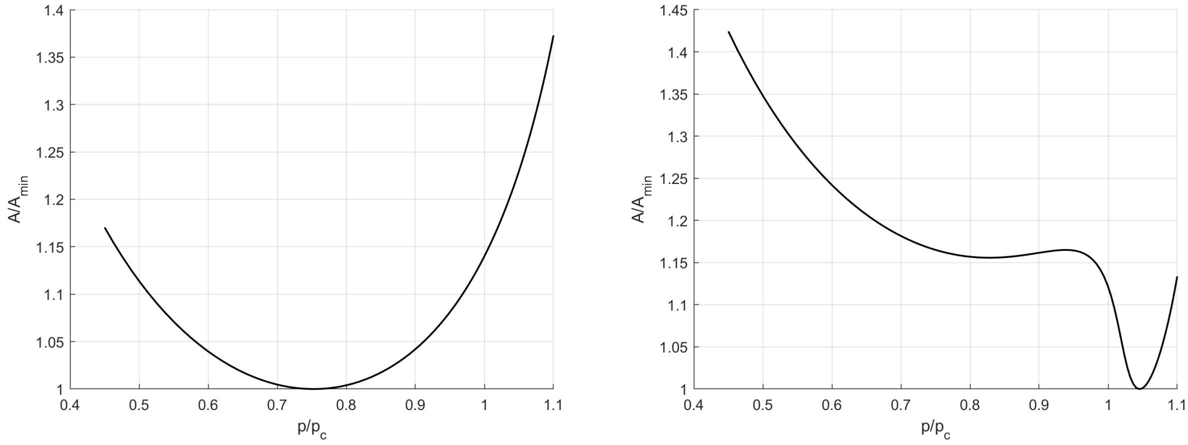

(a) Area, Ideal Gas Model

(b) Area, Van der Waals Gas Model

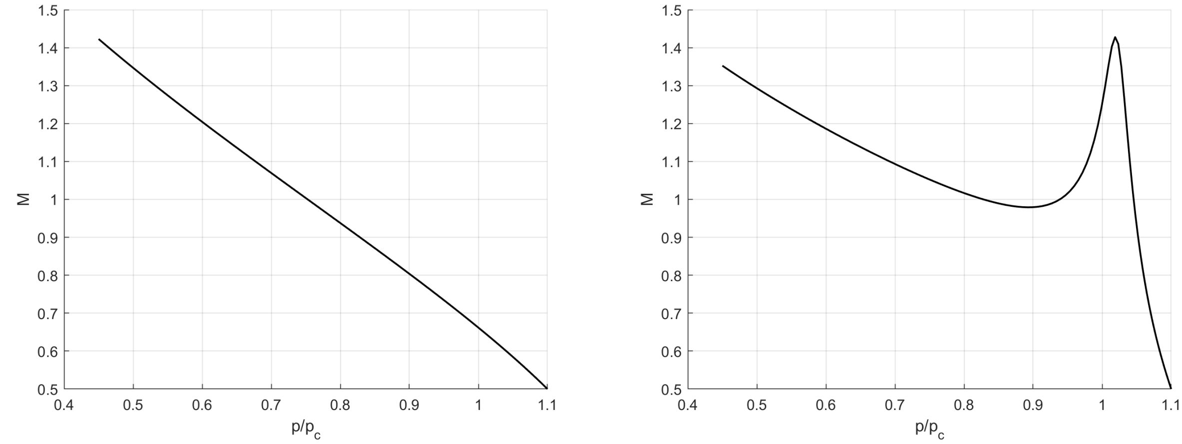

(c) Mach number, Ideal Gas Model

(d) Mach number, Van der Waals Gas Model

Figure 4.4: Cross-sectional area ratio and Mach number distribution (Case 1)

smaller than 0. According to equation (3.54), a divergent-convergent part will be needed. In Figure 4.4b at around $p/p_c = 0.95$, it is clearly shown that there is a local maximum point corresponding with $M = 1$.

Figures 4.5a and 4.5b show the speed of sound distribution in comparison with the ideal-gas model. The classical theory states that the speed of sound is a function of temperature only

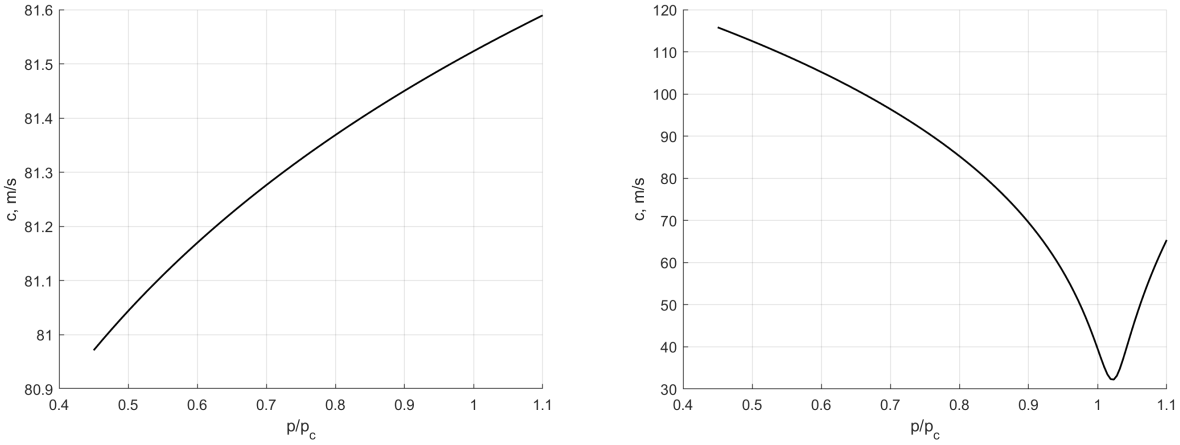

(a) Ideal Gas Model (b) Van der Waals Gas Model

Figure 4.5: Speed of sound (Case 1)

and increases with pressure increasing monotonically, while equation (2.9) shows that

$$\Gamma - 1 = \frac{c}{v}\left(\frac{\partial c}{\partial p}\right)_s$$

For a non-conventional gas flow when Γ is no longer a constant larger than 1, how the speed of sound changes with pressure depends on the value of Γ. When Γ goes below 1, the speed of sound decreases with increasing pressure, which is opposite to the classical theory.

Figures 4.6, 4.7, and 4.8 plot the analogous distribution of temperature, density and velocity along the isentrope, respectively. The outlet temperature by using Van der Waals equation does not go as low as the ideal-gas one. The reason causing this difference is that the ideal-gas law treats the molecules of a gas as point particles with perfectly elastic collisions, while the Van der Waals model takes into account molecular size and molecular interaction forces. So, more internal energy is contained and thus the temperature at the same location will be higher than the ideal-gas model.

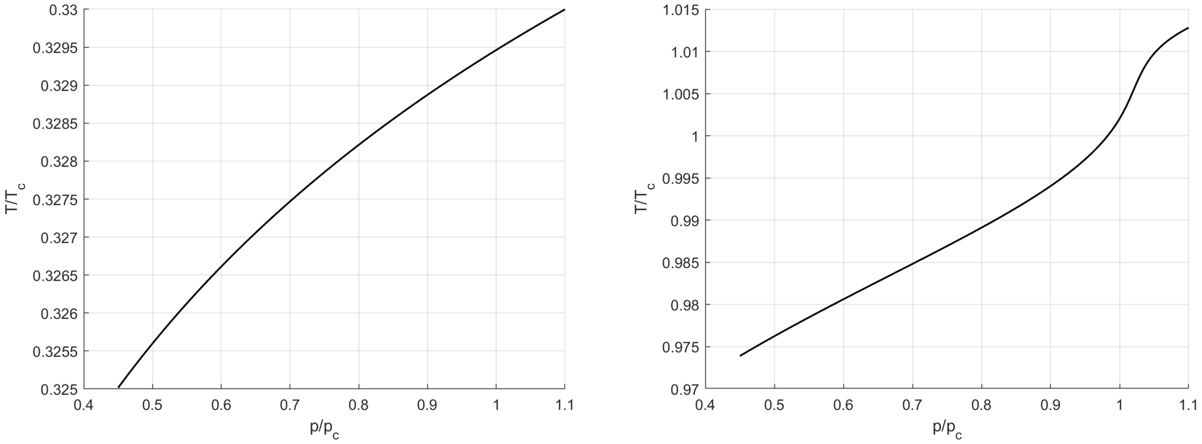

(a) Ideal Gas Model

(b) Van der Waals Gas Model

Figure 4.6: Temperature distribution (Case 1)

Regarding the curvature change of density in Van der Waals model results, recall the definition of Γ, equation (2.1)

$$\Gamma = \frac{c^4}{2v^3}\left(\frac{\partial^2 v}{\partial p^2}\right)_s$$

It states that the curvature of the density function is related to the sign of Γ. For an ideal gas, Γ is always a positive number which leads to positive $\left(\frac{\partial^2 v}{\partial p^2}\right)_s$. But for a non-conventional gas, it will cause the density function turning from concave to convex at the $\Gamma = 0$ point.

The velocity function of the flow does not show a significant difference as previous variables. But the velocity increment from Van der Waals model results is higher than ideal-gas results.

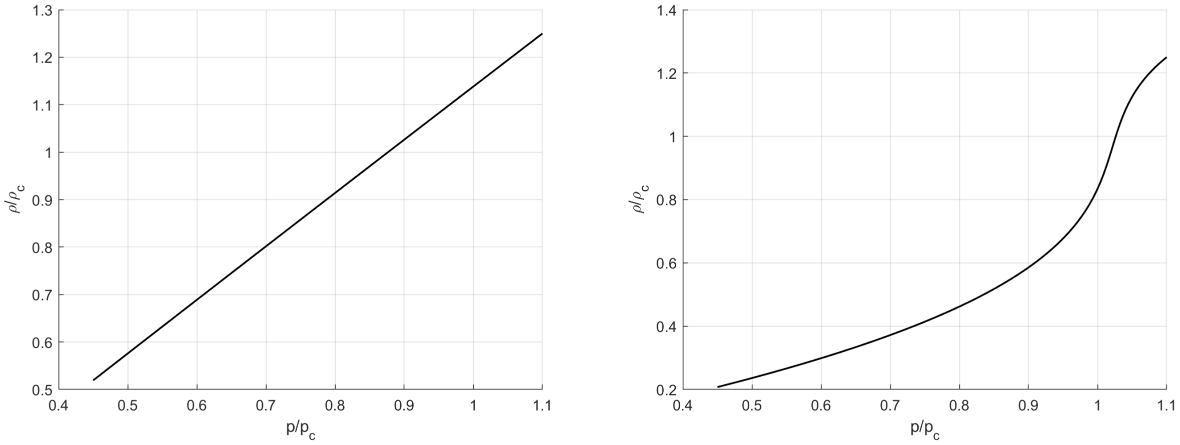

(a) Ideal Gas Model

(b) Van der Waals Gas Model

Figure 4.7: Density distribution (Case 1)

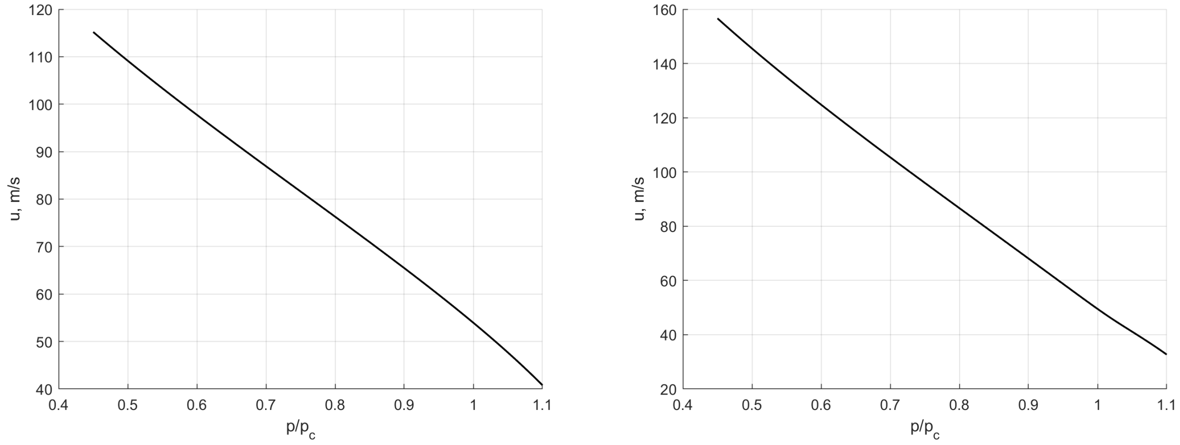

(a) Ideal Gas Model

(b) Van der Waals Gas Model

Figure 4.8: Velocity distribution (Case 1)

4.3 Isentropic Flow with Supersonic Inlet Condition

To keep the isentropic process staying close to the saturation line and critical point, the same pressure profile and upstream condition with the previous case was imposed besides that the inlet Mach number is increased to 3. The gas is expanded further more than the subsonic case until $p = 0.1p_c$. Here distributions of the same variable calculated by the ideal-gas equation of state and Van der Waals model are plotted together to save space.

Figure 4.9a plots the fundamental derivative versus pressure along this isentropic process, and displays the same trend as in the subsonic case. Γ stays in the negative area from around $p/p_c = 0.88$ to $p/p_c = 1.02$. At the end of the nozzle, Γ is slightly less than 1.

Figures 4.9 and 4.10 plot the distribution of cross-sectional area, Mach number, speed of sound, temperature, density, velocity, and non-dimensional variables A and B of the supersonic case. Similar results with the subsonic case are obtained. The ideal-gas relations cannot give accurate results here when the isentrope is close to the saturation line. The main differences between Van der Waals model results and ideal-gas theory are given below.

- The Mach number is no longer a monotonic function of pressure. With decreasing pressure, it jumps to values larger than 6 and then decreases rapidly within the negative fundamental derivative region. With further lowering of the pressure, it rises slowly but remains smaller than the Mach number from ideal-gas law.
- Much larger cross-sectional area ratio is needed to achieve the same pressure drop. Here at the outlet of the nozzle, the area ratio is about two times the ideal-gas result.
- The speed of sound does not change too much in the ideal-gas case, whereas the ratio of c_{max} to c_{min} is larger than 3 in the Van der Waals model results. The velocity distribution displays the same trend as in the ideal-gas results, but the values of velocity grow more rapidly than the velocity in ideal-gas case.

- Under the same pressure drop, the temperature ratio is significantly larger than the ideal-gas case while the density ratio is just slightly larger. The larger temperature indicates that the gas contains more internal energy.

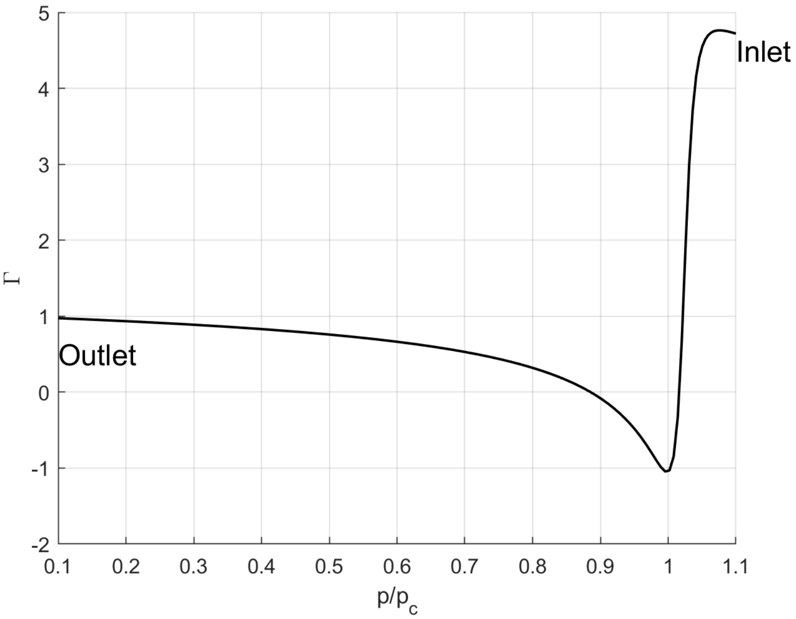

(a) Fundamental derivative

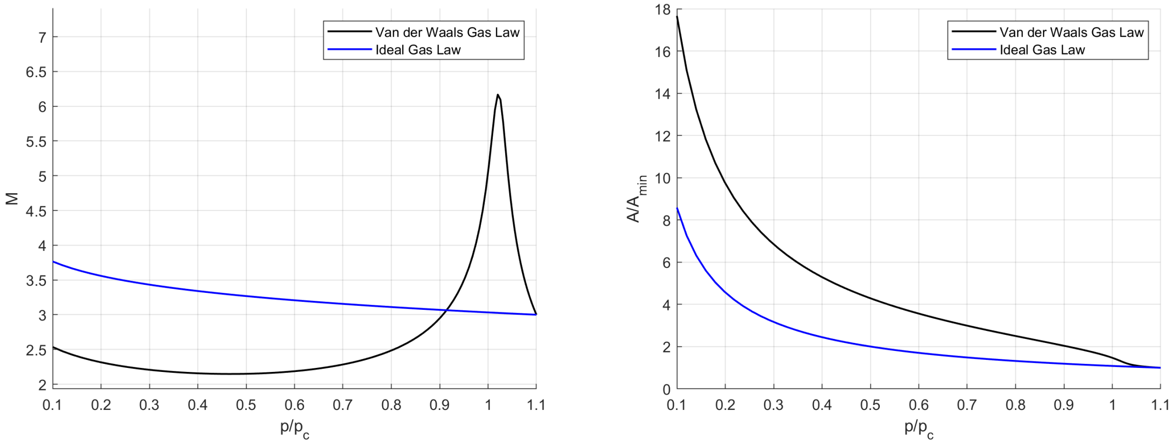

(b) Mach number

(c) Cross-sectional area ratio

Figure 4.9: Case 2: $p_{in} = 1.1p_c, M_{in} = 3, v_{in} = 0.8v_c$

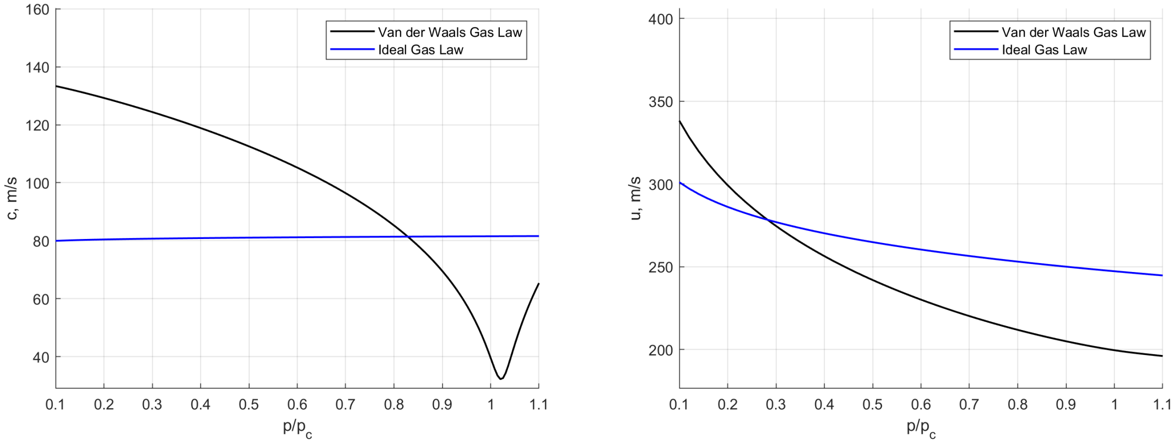

(a) Speed of sound (b) Velocity

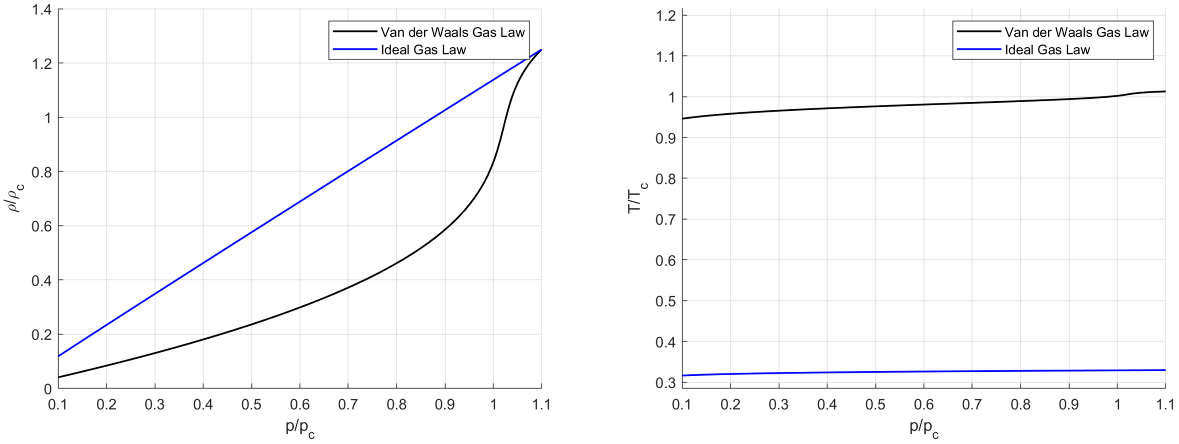

(c) Density (d) Temperature

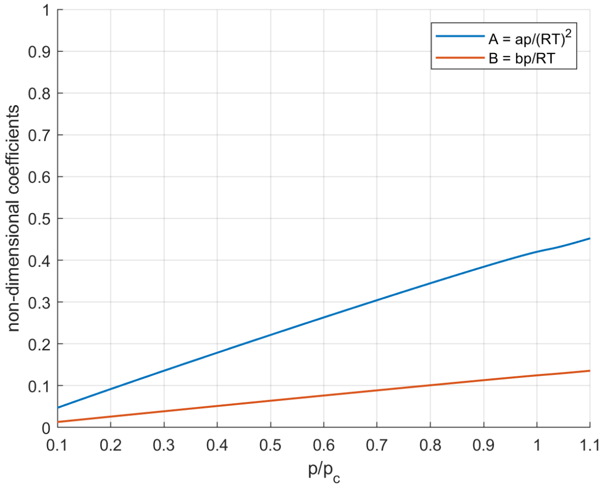

(e) Variation of non-dimensional variables A and B

Figure 4.10: Case 2: $p_{in} = 1.1p_c, M_{in} = 3, v_{in} = 0.8v_c$ (Continued)

Chapter 5

Conclusion

Unconventional gas behavior in isentropic quasi-one-dimensional flow has been investigated in the present work. The sign and value of the fundamental derivative Γ significantly influence the gas behavior and flow properties. For dense gas, there are certain regions that the flow behavior is different from ordinary gas-dynamics and it should be noted that these phenomena usually appear simultaneously. Once the region of negative fundamental derivative is located, interesting unconventional gas behaviors are explored, demonstrated, and analyzed.

When $\Gamma < 1$, the speed of sound decreases with increasing gas pressure, and the Mach number is no longer a monotonic function of velocity. Mach number increases with velocity only for $M^2 < \dfrac{1}{1-\Gamma}$. When $\Gamma < 0$, the results from classical theory are inverted. To create transonic flow, a divergent-convergent nozzle is needed instead of the traditional convergent-divergent nozzle. Along with the increasing cross-sectional area ratio, the Mach number increases in subsonic flow and decreases in supersonic flow.

Besides these qualitative differences, comparing with the ideal-gas relations, the changes of the cross-sectional area ratio, the speed of sound, the velocity and the temperature are significantly larger to achieve the same pressure drop in an isentropic flow. A dense gas called MDM is used as the working fluid, and the Van der Waals model is applied in the computations of the present work.

The understanding of the physical meaning of these unconventional phenomena in quasi-1D isentropic flow is leading us to the next step of this study, including but not limited to the non-ideal gas behavior in one-dimensional Fanno flow and Rayleigh flow, the general jump relation of normal shock wave, the formation of a Prandtl-Mayer wave and nonlinear wave propagation, and further investigation in two-dimensional oblique shock. More results will be reported in the near future. These analyses will provide us with needed insight into the physics of such non-classical flow phenomena and preparation for numerical computation of such flows in more general two- and three-dimensional axial compressors.

For future work beyond this Master's thesis, the plan is to implement the unconventional gas flow theory into our in-house code to perform numerical simulations under realistic conditions and with realistic geometric configurations. Flat plate flow and two-dimensional cascade flow will be calculated and viscosity will be taken into consideration. Different gas models and numerical schemes will be compared. It is hoped that these computation results will later be validated with experimental data and provide feedback for developing a robust and sophisticated turbo-machinery design tool.

Bibliography

[1] Yoonhan Ahn, Seong Jun Bae, Minseok Kim, Seong Kuk Cho, Seungjoon Baik, Jeong Ik Lee, and Jae Eun Cha. Review of supercritical co2 power cycle technology and current status of research and development. *Nuclear Engineering and Technology*, 47(6):647–661, 2015.

[2] Vaclav Dostal, Pavel Hejzlar, and Michael J Driscoll. The supercritical carbon dioxide power cycle: comparison to other advanced power cycles. *Nuclear technology*, 154(3):283–301, 2006.

[3] Junhyun Cho, Munkyoung Choi, Young-Jin Baik, Gilbong Lee, Ho-Sang Ra, Byunghui Kim, and Minsung Kim. Development of the turbomachinery for the supercritical carbon dioxide power cycle. *International Journal of Energy Research*, 40(5):587–599, 2016.

[4] Enrico Rinaldi, Rene Pecnik, and Piero Colonna. Computational fluid dynamic simulation of a supercritical co2 compressor performance map. *Journal of Engineering for Gas Turbines and Power*, 137(7):072602, 2015.

[5] Nikola D Baltadjiev, Claudio Lettieri, and Zoltán S Spakovszky. An investigation of real gas effects in supercritical co2 centrifugal compressors. *Journal of Turbomachinery*, 137(9):091003, 2015.

[6] Hans Albrecht Bethe. The theory of shock waves for an arbitrary equation of state, office of scientific research and development, washington. *Report*, 575:57, 1942.

[7] P Duhem. On the propagation of shock waves in fluids. *Z. Phys. Chem*, 69:169–186, 1909.

[8] Hermann Weyl. Shock waves in arbitrary fluids. *Communications on Pure and Applied Mathematics*, 2(2-3):103–122, 1949.

[9] Richard Courant and Kurt Otto Friedrichs. *Supersonic flow and shock waves*, volume 21. Springer Science & Business Media, 1999.

[10] Lev Davidovich Landau and Evgenii Mikhailovich Lifshits. *Fluid mechanics, by LD Landau and EM Lifshitz*, volume 11. Pergamon Press Oxford, UK, 1959.

[11] Philip A Thompson. A fundamental derivative in gasdynamics. *The Physics of Fluids*, 14(9):1843–1849, 1971.

[12] MS Cramer and GM Tarkenton. Transonic flows of bethe-zel'dovich—thompson fluids. *Journal of Fluid Mechanics*, 240:197–228, 1992.

[13] Hugh Longbourne Callendar. On the thermodynamical properties of gases and vapours as deduced from a modified form of the joule-thomson equation, with special reference to the properties of steam. *Proceedings of the Royal Society of London*, 67(435-441):266–286, 1901.

[14] DA Sullivan. Historical review of real-fluid isentropic flow models. *Journal of Fluids Engineering*, 103(2):258–267, 1981.

[15] V Arp, JM Persichetti, and Guo-bang Chen. The gruneisen parameter in fluids. *Journal of fluids engineering*, 106(2):193–200, 1984.

[16] E Grüneisen. Zustand des festen körpers. In *Thermische Eigenschaften der Stoffe*, pages 1–59. Springer, 1926.

[17] JC Leung and M Epstein. A generalized critical flow model for nonideal gases. *AIChE journal*, 34(9):1568–1572, 1988.

[18] Robert C Johnson. Calculations of real-gas effects in flow through critical-flow nozzles. *Journal of Basic Engineering*, 86(21):519–526, 1964.

[19] W Bober and WL Chow. Nonideal isentropic gas flow through converging-diverging nozzles. *Journal of fluids engineering*, 112(4):455–460, 1990.

[20] William A Sirignano. Normal shocks with high upstream pressure. *Physical Review Fluids*, 3(9):093401, 2018.

[21] William A Sirignano. Compressible flow at high pressure with linear equation of state. *Journal of Fluid Mechanics*, 843:244–292, 2018.

[22] Piero Colonna and Paolo Silva. Dense gas thermodynamic properties of single and multicomponent fluids for fluid dynamics simulations. *J. Fluids Eng.*, 125(3):414–427, 2003.

[23] G Angelino and C Invernizzi. Cyclic methylsiloxanes as working fluids for space power cycles. 1993.

[24] Alberto Guardone, Piero Colonna, Emiliano Casati, and Enrico Rinaldi. Non-classical gas dynamics of vapour mixtures. *Journal of fluid mechanics*, 741:681–701, 2014.

[25] Hans Albrecht Bethe. On the theory of shock waves for an arbitrary equation of state. In *Classic papers in shock compression science*, pages 421–495. Springer, 1998.

[26] P Cinnella, PM Congedo, and D Laforgia. Transonic flows of bzt fluids through turbine cascades. In *Computational Fluid Dynamics 2004*, pages 227–232. Springer, 2006.

[27] MS Cramer. Nonclassical dynamics of classical gases. In *Nonlinear waves in real fluids*, pages 91–145. Springer, 1991.

[28] Luuc Keulen, Elisabeth Mansfield, Ian H Bell, Andrea Spinelli, and Alberto Guardone. Bubble-point measurements and modeling of binary mixtures of linear siloxanes. *Journal of Chemical & Engineering Data*, 63(9):3315–3330, 2018.

[29] Dimitrios A Kouremenos and Xenofon K Kakatsios. The three isentropic exponents of dry steam. *Forschung im Ingenieurwesen A*, 51(4):117–122, 1985.

[30] Pim Nederstigt. Real gas thermodynamics: and the isentropic behavior of substances. 2017.

[31] H Gray Funkhouser. A short account of the history of symmetric functions of roots of equations. *The American mathematical monthly*, 37(7):357–365, 1930.

Appendix A

Thermodynamic Identities

A.1 Exact Differential and Triple Product Rule

In thermodynamics, there's a set of equations that are derived by application of Euler's reciprocity relation to the thermodynamic characteristic functions. Consider a function described by three variables $F = F(x, y, z)$. It can be differentiated as

$$dF = Adx + Bdy + Cdz \tag{A.1}$$

The exactness criteria for this function states that

$$\left(\frac{\partial A}{\partial y}\right)_{x,z} = \left(\frac{\partial B}{\partial x}\right)_{y,z} \tag{A.2}$$

$$\left(\frac{\partial A}{\partial z}\right)_{x,y} = \left(\frac{\partial C}{\partial x}\right)_{y,z} \tag{A.3}$$

$$\left(\frac{\partial B}{\partial z}\right)_{x,y} = \left(\frac{\partial C}{\partial y}\right)_{x,z} \tag{A.4}$$

where the three variables are related by the triple product relation

$$\left(\frac{\partial x}{\partial y}\right)_z \left(\frac{\partial y}{\partial z}\right)_x \left(\frac{\partial z}{\partial x}\right)_y = -1 \tag{A.5}$$

A.2 Maxwell Relations

The general form of Gibbs equation gives that

$$du = Tds - pdv \tag{A.6}$$

$$dh = vdp + Tds \tag{A.7}$$

By applying exactness criteria, the four most common Maxwell relations are

$$\left(\frac{\partial T}{\partial v}\right)_s = -\left(\frac{\partial p}{\partial s}\right)_v \tag{A.8}$$

$$\left(\frac{\partial T}{\partial p}\right)_s = \left(\frac{\partial v}{\partial s}\right)_p \tag{A.9}$$

$$\left(\frac{\partial s}{\partial v}\right)_T = \left(\frac{\partial p}{\partial T}\right)_v \tag{A.10}$$

$$\left(\frac{\partial s}{\partial p}\right)_T = -\left(\frac{\partial v}{\partial T}\right)_p \tag{A.11}$$

A.3 Derivation of Equation (2.10)

Equation (2.5) states that

$$\Gamma = \frac{v^3}{2c^2}\left(\frac{\partial^2 p}{\partial v^2}\right)_s$$

To derive $\left(\frac{\partial^2 p}{\partial v^2}\right)_s$ in terms of thermodynamic state variables, start with the first order derivative along the isentrope $\left(\frac{\partial p}{\partial v}\right)_s$.

$$
\begin{aligned}
\left(\frac{\partial p}{\partial v}\right)_s &= -\left(\frac{\partial p}{\partial s}\right)_v \left(\frac{\partial s}{\partial v}\right)_p \\
&= \left(\frac{\partial T}{\partial v}\right)_s \left(\frac{\partial p}{\partial T}\right)_s \\
&= \left(\frac{\partial T}{\partial s}\right)_v \left(\frac{\partial s}{\partial v}\right)_T \left(\frac{\partial p}{\partial s}\right)_T \left(\frac{\partial s}{\partial T}\right)_p \\
&= -\frac{T}{c_v} \left(\frac{\partial p}{\partial T}\right)_v \left(\frac{\partial T}{\partial v}\right)_p \frac{c_p}{T} \\
&= -\frac{c_p}{c_v} \left(\frac{\partial v}{\partial T}\right)_p \left(\frac{\partial p}{\partial v}\right)_T \left(\frac{\partial p}{\partial v}\right)_T \left(\frac{\partial T}{\partial p}\right)_v \\
&= -\left[1 + \frac{T}{c_v} \left(\frac{\partial v}{\partial T}\right)_p \left(\frac{\partial p}{\partial T}\right)_v\right] \left[\left(\frac{\partial v}{\partial T}\right)_p \left(\frac{\partial p}{\partial v}\right)_T^2 \left(\frac{\partial T}{\partial p}\right)_v\right] \\
&= \left(\frac{\partial p}{\partial v}\right)_T + \frac{T}{c_v} \left(\frac{\partial v}{\partial T}\right)_p \left(\frac{\partial p}{\partial T}\right)_v \left(\frac{\partial p}{\partial v}\right)_T \\
&= \left(\frac{\partial p}{\partial v}\right)_T - \frac{T}{c_v} \left(\frac{\partial p}{\partial T}\right)_v^2
\end{aligned}
$$

Then another differentiation gives

$$\begin{aligned}
\left(\frac{\partial^2 p}{\partial v^2}\right)_s &= \left(\frac{\partial\left(\left(\frac{\partial p}{\partial v}\right)_T - \frac{T}{c_v}\left(\frac{\partial p}{\partial T}\right)_v^2\right)}{\partial v}\right)_s \\
&= \underbrace{\left(\frac{\partial\left(\left(\frac{\partial p}{\partial v}\right)_s\right)}{\partial v}\right)_T}_{\text{①}} - \frac{1}{c_v}\left(\frac{\partial p}{\partial T}\right)_v^2 \underbrace{\left(\frac{\partial T}{\partial v}\right)_s}_{\text{②}} + \frac{T}{c_v^2}\left(\frac{\partial p}{\partial T}\right)_v^2 \underbrace{\left(\frac{\partial c_v}{\partial v}\right)_s}_{\text{③}} \\
&\quad - \frac{2T}{c_v}\left(\frac{\partial p}{\partial T}\right)_v \underbrace{\left(\frac{\partial\left(\left(\frac{\partial p}{\partial v}\right)_s\right)}{\partial T}\right)_v}_{\text{④}}
\end{aligned}$$

The four terms marked in the equation above are derived below. To keep the expression elegant, here $\partial/\partial T$ implies that v is kept constant, and vice versa.

$$\begin{aligned}
\text{①} &= \frac{\partial^2 p}{\partial v^2} + \frac{T}{c_v^2}\left(\frac{\partial p}{\partial T}\right)^2 \frac{\partial c_v}{\partial v} - \frac{2T}{c_v}\frac{\partial p}{\partial T}\frac{\partial^2 p}{\partial v \partial T} \\
\text{②} &= -\frac{T}{c_v}\frac{\partial p}{\partial T} \\
\text{③} &= \frac{\partial c_v}{\partial v} - \frac{T}{c_v}\frac{\partial p}{\partial T}\frac{\partial c_v}{\partial T} \\
\text{④} &= \frac{\partial^2 p}{\partial v \partial T} - \frac{1}{c_v}\left(\frac{\partial p}{\partial T}\right)^2 + \frac{T}{c_v^2}\left(\frac{\partial p}{\partial T}\right)^2 \frac{\partial c_v}{\partial T} - \frac{2}{c_v}\frac{\partial p}{\partial T}\frac{\partial c_v}{\partial v}
\end{aligned}$$

Substitute the above expressions back into $\left(\frac{\partial^2 p}{\partial v^2}\right)_s$ and reorganize the equation, we obtain

$$\left(\frac{\partial^2 p}{\partial v^2}\right)_s = \frac{\partial^2 p}{\partial v^2} - \frac{3T}{c_v}\frac{\partial p}{\partial T}\frac{\partial^2 p}{\partial v \partial T} + \left(\frac{T}{c_v}\frac{\partial p}{\partial T}\right)^2 \left[\frac{3}{T}\frac{\partial c_v}{\partial v} + \frac{1}{T}\frac{\partial p}{\partial T}\left(1 - \frac{T}{c_v}\frac{\partial c_v}{\partial T}\right)\right] \qquad \text{(A.12)}$$